

The Collatz function as an automorphic Cayley colour graph: decidability of $an+b$ conjectures, proof of the $3n + 1$ conjecture

Jan Kleinnijenhuis¹ and Alissa M. Kleinnijenhuis²

¹Vrije Universiteit Amsterdam, The Network Institute

j.kleinnijenhuis@vu.nl

²Cornell University,

alissa.kleinnijenhuis@cornell.edu

April 12, 2024

Abstract

The Collatz conjecture states that repeated steps of $n \rightarrow 3n+1$ at odd numbers and $n \rightarrow n/2$ at even numbers amount to walks over root paths to the branching number $c = 4$ in the ‘trivial’ cyclic root $4 \rightarrow 2 \rightarrow 1 \rightarrow 4 \rightarrow \dots$ of one connected Collatz graph. The Collatz graph with reverse arrows $n \rightarrow 2n$ and $n \rightarrow (n-1)/3$ can be transformed to a 3-regular automorphic Cayley color graph $T_{\geq 0}$ with as nodes the branching numbers with a remainder of 4 or 16 when divided by 18, building the congruence classes $[4, 16]_{18}$. Labeling the 2^k breadth-first ordered root paths with 2^k binary numbers on the binary number line, for $k = 1, 2, 3, \dots$, and pairing them with the 2^k output numbers of these root paths, gives 2^k paired numbers. The 3-regular Cayley graph of these paired branching numbers can be transformed to a 4-regular Middle Pages graph. This 4-regular graph offers to all paired branching numbers from the congruence classes $[4, 16]_{18}$ a unique Eulerian round tour to and from the trivial root number pair $_{c=4}^0$. This proves Collatz’s $3n + 1$ conjecture. Whether a specific $an + b$ conjecture offers a Eulerian round tour to all its paired branching numbers can be decided by whether it offers such a tour to paired branching numbers lower than $2a^3$.

1	Introduction	2
2	Proof Approach	6
3	Transformations of the Collatz graph G_C and the 3-regular Cayley colour graph $T_{\geq 0}$	12
4	The 4-regular middle pages graph G_{MP}	24
5	The Collatz congruence classes graph $G_{CC} = ([0, \dots, 17]_{18}, [f, g])$	26
6	Discussion	39

1 Introduction

The Collatz function C returns $n \rightarrow n/2$ arrows for even numbers and $n \rightarrow 3n + 1$ arrows for odd numbers [1]. Its iterations can be represented as *paths* of concatenated arrows, allowing for a *walk* of successive steps. The Collatz conjecture to be proven maintains that iterations of the Collatz function give each natural number a *root path* converging to the cyclic *trivial root trajectory* $\cdots \rightarrow (4 \rightarrow 2 \rightarrow 1 \rightarrow 4 \rightarrow \cdots)$, with $c = 4$ as first and last number in each cycle. The illustration below for 9, 7, and 8 shows that the root path of 9 to the trivial root converges to that of 7, which converges to that of 8, which converges to $c = 4$ in the trivial root.

Example 1.1. Three root paths converging to the trivial root number $c = 4$

$7 \rightarrow 22 \rightarrow 11 \rightarrow 34 \rightarrow 17 \rightarrow 52 \rightarrow 26 \rightarrow 13 \rightarrow 40 \rightarrow 20 \rightarrow 10 \rightarrow 5 \rightarrow 16 \rightarrow (8 \rightarrow \cdots)$
 $8 \rightarrow (4 \rightarrow 2 \rightarrow 1 \rightarrow 4 \rightarrow \cdots)$.
 $9 \rightarrow 28 \rightarrow 14 \rightarrow (7 \rightarrow \cdots)$

The brackets $()$ enclose the continuation of a root path. The red arrows highlight $n \rightarrow 3n + 1$ expansions for odd numbers. The term 'wondrous numbers' [2, 3] indicates that natural numbers have wondrously ordered root paths and that successive numbers have very different 'not obviously simple' [2] root paths, just as successive numbers have very different prime factorisations, e.g. $7 \rightarrow 7, 8 \rightarrow 2^3, 9 \rightarrow 3^2$. Nevertheless root paths appear to converge, to a single connected tree [4, ch.3] anchored at the branching number $c = 4$ in the trivial root trajectory including the lowest natural number 1.

Fig. 1a of the Collatz graph G_C shows short root paths in the tree rooted in $c = 4$, including root paths of numbers as high as 5440, 5460, 5461, and also 16384 and 32768 on the most rightist root path labeled the *upward trunk*. The most leftist root path, labeled as the *greedy branch* [5, Seq.A225570], with 22 on it is also shown but not the root paths of the even lower numbers 7 and 9 that converge to it (Example 1.1).

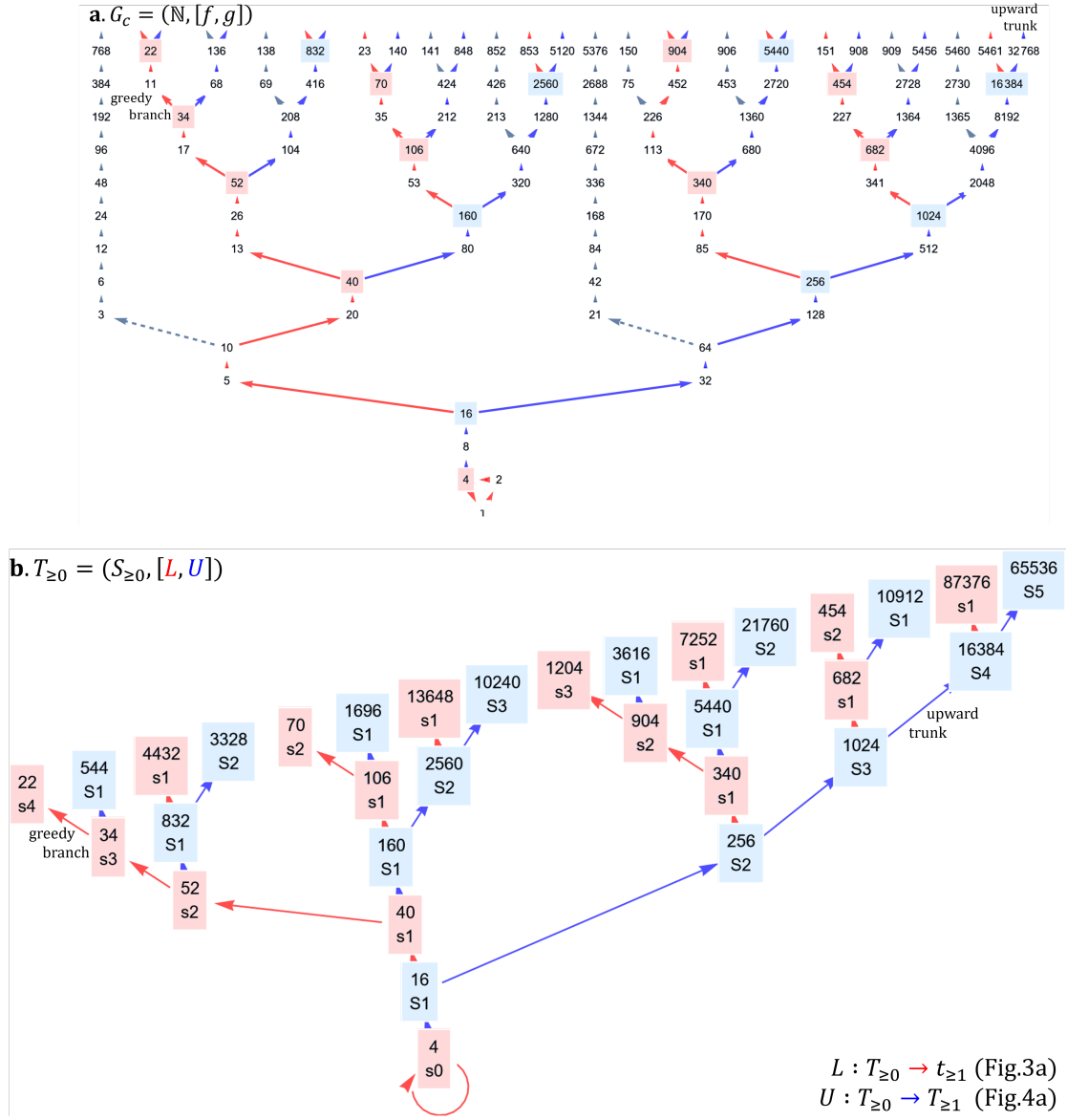
Fig. 1b simplifies branching patterns in the Collatz graph G_C by its transformation to a 3-regular graph (Def. 1.2) with one parent and two children for each of its nodes, labelled as the Cayley colour graph $T_{\geq 0}$.

Definition 1.2. A regular graph. A directed graph is *regular* if all its nodes have the same *indegree* and the same *outdegree*, i.e. the same number of incoming arrows, and of outgoing arrows [4]. A regular graph is k -regular if the number of incoming and outgoing arrows is k for all its nodes.

Each node in the Cayley graph has a red-coloured arrow to a leftward child defined by the leftward function $L : (n - 1)/3 \cdot 2^j$ with a $f : n \rightarrow (n - 1)/3$ step first and $g : n \rightarrow 2n$ steps next (Def. 5.2), and also a blue-coloured arrow to an upward child $U : n \rightarrow n \cdot 2^j$ of g steps only (Def. 5.1), for $1 \leq i, j \leq 4$. The Cayley graph $T_{\geq 0}$ retains from the Collatz graph G_C branching numbers with both red- and blue-coloured successors, thereby retaining from the previously mentioned numbers 4, 22, 16384 and 5440. Fig. 1b shows the lowest $k = 5$ breadth-first levels of the Cayley graph with root paths of $2^k = 32$ branching numbers, of which $2^k - 1 = 16$ at level $k = 5$.

Our proof approach (section 2, Fig. 2) is that the transformation of graph G_C (Fig. 1a) to $T_{\geq 0}$ (Fig. 1b), detailed in section 3, enables subsequent transformations [6, 7, 8, 9, 10] that prove the Collatz conjecture. What will be proved is that there are no numbers that converge to trees anchored in a non-trivial root trajectory, with perhaps a colossally high lowest number X (Col. 5.15). This could either be a *non-trivial cycle* next to the trivial cycle, or a *diverging trajectory* with gradually higher instead of gradually lower numbers [11]. A non-trivial root trajectory could sustain a forest of trees, one anchored in each of its branching numbers. The Collatz problem, therefore, resembles the halting problem posed by Alan Turing (1912-1954) [12] whether a computer program will terminate as expected in finite time regardless of its specific input, or whether it could either be trapped in an infinite cyclic loop or in diverging computations with ever higher numbers [12, 13].

Figure 1: **a.** The Collatz graph G_C and **b.** its regular Cayley colour graph $T_{\geq 0}$



Legend | a: G_C . An upward path $U : n \rightarrow n \cdot 2^p$ of $g : n \rightarrow 2n$ arrows (blue) connects each branching number to an upward child, e.g. $U : 16 \rightarrow 32 \rightarrow 64 \rightarrow 128 \rightarrow 256$ (blue). A leftward path $L : n \rightarrow (n-1)/3 \cdot 2^q$ (red) connects each branching number via an $f : n \rightarrow (n-1)/3$ arrow to a leftward child, e.g. $L : 16 \rightarrow 5 \rightarrow 10 \rightarrow 20 \rightarrow 40$ (red). Uncoloured numbers either do not branch, or have non-branching successors divisible by 3 (grey line graphs).

b: $T_{\geq 0}$. In the 3-regular colour graph $T_{\geq 0} = (S_{\geq 0}, [L, U])$, paths of arrows to upward and leftward children become arrows, e.g. $U : 16 \rightarrow 256$ and $L : 16 \rightarrow 40$. Each branching number is the *foot number* of a V-shaped graph with on its *V-arms* upward successors of its leftward child in upward generations S_1, S_2, S_3, \dots , e.g.

$LU^{1,2,3,\dots} : 16 \rightarrow 40 \rightarrow 160_{S1} \rightarrow 2560_{S2} \rightarrow 10240_{S3} \rightarrow \dots$ and leftward successors of its upward child in leftward generations s_1, s_2, s_3, \dots , e.g. $UL^{1,2,3,\dots} : 16 \rightarrow 256 \rightarrow 340_{s1} \rightarrow 904_{s2} \rightarrow 1204_{s3} \rightarrow \dots$. Each V-arm number is also the foot number of its own V-graph. The branching root number $c = 4_{s0}$ is its own parent. |

1.1 Literature review

Term rewriting approaches [14, 15] and Hydra games [16] offer heuristic arguments in favour of the Collatz conjecture. Fields medallist Terence Tao could recently prove that the Collatz conjecture holds for ‘almost all’ numbers [17]. Tao sets up a two-stage proof for even numbers and odd numbers. Since repeated $n/2$ divisions bring each even number to an odd number, Tao uses the Syracuse function on odd numbers $f_S : n \rightarrow (n+1)/2^q$, in which q is the lowest exponent that gives an odd number as function value f_S . The not depicted *Syracuse graph* of exclusively odd numbers results with more complex branching patterns than the Collatz graph itself. The Syracuse graph is irregular, since odd numbers o do not share the same outdegree, as can be seen in Fig.1a. Depending on whether o is divisible by 3, odd numbers have no odd successors (e.g. 3, 69, 141, 213, ...) or infinitely many odd successors $f : o \rightarrow (o^p - 1)/3$, for $p \in 1, 2, 3, \dots$. For example, Fig.1a reveals that the unique infinite odd subset to which the odd number 5 is connected in the Syracuse graph starts with the odd numbers $13(p=3)$, $53(p=5)$, $853(p=9)$, The *periodic density* (Def.1.3) in it of odd numbers appears to be unpredictable.

Definition 1.3. *Periodic density.* Consider all numbers from a set S of k congruence classes $S = [c_i]_m$, where $0 \leq i \leq m-1$, k is the count of distinct classes c_i , and m is the periodicity or modulus. Their *periodic density*, abbreviated as d , is defined as $d = k/m$. Set S includes k numbers out of each set of m consecutive natural numbers.

The definition of periodic density (Def.1.3) captures that out of every successive range of 2 numbers one is odd ($d = 1/2$), while out of every successive range of 3 numbers one is divisible by 3 ($d = 1/3$) and two are not ($d = 2/3$), and so on. This periodic density measure (Def.1.3) tells the maximum density $d = 3/6 = 1/2$ of odd numbers $[1, 3, 5]_6$ in the Syracuse graph, and the maximum density $d = 2/6$ of odd numbers $[1, 5]_6$ not divisible by 3 in it. Although Tao leaves out numbers divisible by 3 from the interesting part of the density calculations ([18, Prop.1.17,p.11]), Tao uses instead of a periodic density measure a *logarithmic density* measure, which reveals that ‘almost all’ odd numbers are included in it. Tao concludes that ‘the full resolution of the conjecture remains well beyond current methods’ [17].

Alex Kontorovich, who studied next to Collatz’s $n \rightarrow 3n+1$ -function the $n \rightarrow 5n+1$ -function, which does not let converge all numbers to the trivial root [19], comments to Tao’s ‘almost all’ proof that it may have exceptions (i.e., numbers without a root path to $n=1$) or be *undecidable* [18].

Decidability is easily explained with a high school-level decidability question. Can it be decided whether a parabolic function $y = ax^2 + bx + c$ has real roots purely on the basis of the parameters a , b and c , such that tracing for each value of x whether it is a real root becomes superfluous? Whether a parabolic function has real roots is decided by whether $b^2 \geq 4ac$. The parameters a , b and c decide, for example, that $y = x^2 + 1$ has no real roots, while $y = x^2$ and $y = x^2 - 1$ have at least one real root.

Undecidability, or unpredictability of the generalized class of $an+b$ -functions for odd numbers, still assuming $n \rightarrow n/2$ for even numbers, was shown by J.H. Conway (1937-2020) in the same 1971 article *Unpredictable Iterations* [20] in which he introduced the generalized class of $an+b$ -functions. Conway was already known as the inventor of the *Game of Life*, in which iterations of functions for generational reproduction give unpredictable positions of black squares amidst eight black or white squares. Conway shows that his Minsky program for testing decidability—or predictability—does not recognise whether an $an+b$ function is ‘defined everywhere’, which is not the case for subfunction f that is undefined if it would have yielded a fraction. The Minsky program also overlooks non-periodicity in $an+b$ functions (Def.1.3).

Does Conway’s undecidability proof of $an+b$ functions since $f : n \rightarrow (n-b)/a$ is not defined everywhere [20, 21] also apply to the transformed 3-regular Cayley colour graph (Fig.1b) in which the red-colored leftward function L and the blue-colored upward function U are defined everywhere? If Conway’s undecidability proof would still hold, then the highest achievable would be convergence tests for ever higher numbers [3, 22], without any hope of ever proving Collatz’s $3n+1$ conjecture [23]. In the

next sections 5 we provide a proof (Cols. 2.4, 5.14) of the decidability test below (Theorem 1.4) for the halting of $an + b$ -functions at the trivial root (Table 2) that is solely based on the parameters a and b .

Theorem 1.4. Decidability test of convergence to the trivial root (to be proven in the next sections) . Consider an $an + b$ function defined by the subfunctions f , g , and the inverse subfunctions f^{-1} and g^{-1} , with a trivial root containing $n = 1$ and the lowest possible branching number $c = a \cdot 1 + b = a + b$.

$$\begin{array}{ll} f^{-1} : n \rightarrow an + b & \text{for every positive odd number } n \text{ from congruence class } [1]_2 \\ g^{-1} : n \rightarrow n/2 & \text{for every positive even number } n \text{ from congruence class } [0]_2 \\ f : n \rightarrow (n - b)/a & \text{if } (n - b)/a \text{ is an odd number, not a fraction with } a \text{ in its nominator} \\ g : n \rightarrow 2n & \text{for every natural number } n \text{ from the congruence classes } [0, 1]_2 \end{array}$$

Whether all root paths, which are concatenations of f^{-1} and g^{-1} arrows, converge to the trivial root number $c = a + b$ for all numbers from the congruence classes $[c]_{2a^2}$ in the range $c < n < 2a^3$, decides whether the root paths of all natural numbers converge to the trivial root number $c = a + b$.

Theorem 1.5. Proof of the Collatz conjecture assuming the decidability test (Theorem 1.4 above). For the $3n + 1$ conjecture the trivial root number is $c = 3 + 1 = 4$. The numbers $[c]_{2a^2}$ from the arithmetic progression 4, 22, 40, 58, ... with periodicity $2a^2 = 18$ in the range $4 < n < 54$ are 22 and 40. Their root paths converge to the trivial root $c = 4$, as they are located on the greedy branch to it, as can be seen from Fig.1, and also from the root path of 7 via 22 and 40 to $c = 4$ in the introductory example 1.1. \square

The proof approach in the next section bets on number theoretical elaborations and on transformations of the Collatz graph (Fig.1a). We refute next to Conway's undecidability other unprovability expectations. 'Hopeless, absolutely hopeless' [1] wrote Paul Erdős (1913–1996), the eminent 20th century mathematician who contributed to, and also liked to talk about "The Book" with the most simple and beautiful proofs of mathematical theorems [24, preface]. In a seminal edited volume, Jeffrey Lagarias points out that the $3n + 1$ conjecture was long considered as an isolated problem, but actually 'cuts across' many different fields of mathematics [11, p.14]. His literature reviews [25] reveal however that none of these fields disposes of the definitions and theorems to provide a simple proof of the Collatz conjecture, or to prove its decidability. Lagarias acquiesces that a proof 'remains unapproachable' [11, p.16], 'Now I know lots more about the problem, I'd say it's still impossible' [26].

Remark 1.6. The numbers in the Syracuse graph with odd numbers divisible by 3 finally left out ([17, Prop.1.17,p.11]) are a transformation of numbers in the 3-regular Cayley graph (Fig.1b), holding odd $(n - 1)/3$ images of even branching nodes. The $(n - 1)/3$ images of the branching classes $[4, 16]_{18}$ give congruence classes $[1, 5]_6$. The arrows in the untransformed Syracuse graph partition the classes $[1, 5]_6$ into a countably infinite number of countably infinite disjoint sets of successors of different odd numbers. It is an open question whether increasing parts of this Syracuse graph can be transformed with only a polynomial increase of resources to the directed prime factorization graph, in which each prime number is connected to *all* higher prime numbers. \square

2 Proof Approach

In *The Motivation and Origin of the $3n + 1$ Problem*, Lothar Collatz (1910–1990) expresses specifically his hope to shed light on the ‘numerous connections between elementary number theory and elementary graph theory’ ‘using the fact that one can picture a number theoretic function $f(n)$ with a directed graph’ where each iteration is drawn with ‘an arrow from n to $f(n)$ ’ [17]. We apply Collatz’s proof approach (Fig. 2) by combining elementary graph theory [4, 27, 28, 29] with elementary number theory [30, 31], using that different composite functions of the arrows in the Collatz graph (Fig. 1a) can be pictured as transformed directed graphs showing arrows from their arguments to their outputs. Proving the Collatz requires different transformations of the Collatz graph (Fig. 1a) as can be seen from the titles of sections and figures, and especially from Figure 2 in this section, which already shows all the graph transformations required.

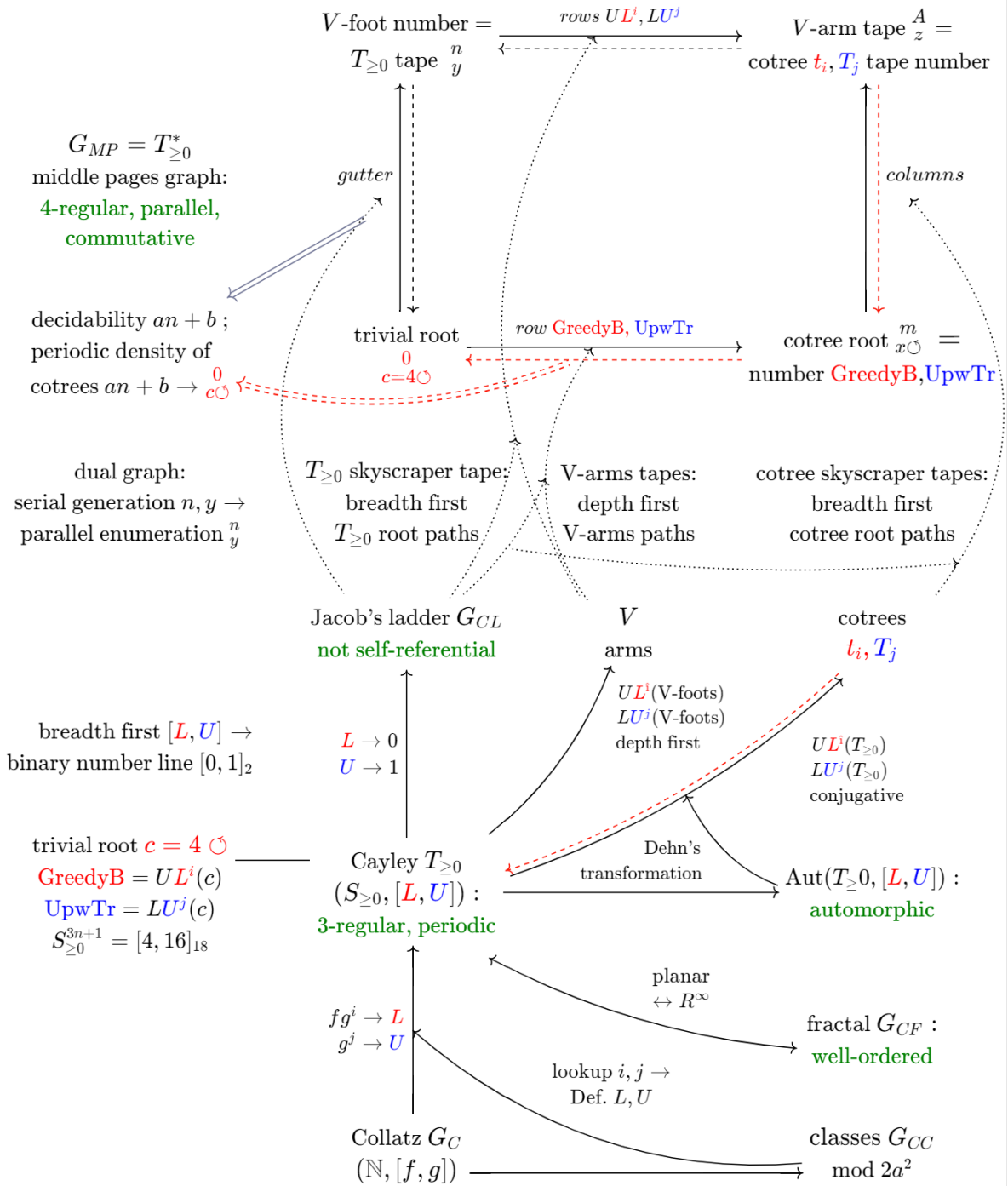
2.1 Elementary number theory

Fig. 2 shows that to arrive at the Cayley graph of all branching numbers (Fig. 1b), the congruence classes graph of an $an + b$ function is required (Section 5, Fig. 10). For the $3n + 1$ function with the Collatz subfunctions $f : n \rightarrow (n - 1)/3$ and $g : n \rightarrow 2n$ this gives as branching numbers $S_{\geq 0} = [4, 16]_{18}$ (Def. 5.2), which are the numbers with a remainder of 4 or 16 after division by their periodicity of $2a^2 = 2 \cdot 3^2 = 18$ (Eq. 5.1). Since 2 out of 18 consecutive numbers are branching numbers, their periodic density (Def. 1.3) is $2/18 = 32/288$.

For each $an + b$ function the periodicity of its branching numbers determines the congruence class contingent powers i and j in the leftward function $L = fg^i$ and in the upward function $U = g^j$ that generate the disjoint sets of red-coloured branching leftward children and blue-coloured branching upward children of branching numbers. For the $3n + 1$ function, both have a periodicity of two gross $2 \cdot 144 = 288$ (Defs. 5.2, 5.1). The specification of the upward and leftward functions is contingent upon congruence classes modulo $2a^2$, respectively congruence subclasses modulo $2a^3$. This amounts for the $3n + 1$ -function to $2 \cdot 3^2 = 18$ distinguishable classes, respectively $2 \cdot 3^2 = 54$ distinguishable subclasses (Fig. 10). The periodic density of branching numbers ($2/18 = 32/288$) can be split in the periodic density of leftward children ($27/288$) and of upward children ($5/288$). The periodic density of leftward and upward children is split in section 5 in the densities of upward and leftward generations S_1, S_2, S_3, \dots and s_1, s_2, s_3, \dots of successors of leftward and upward children. The periodic density of these successors equals the periodic density of all branching numbers generated by the $3n + 1$ function, which does not hold for other functions such as $3n - 1$ and $5n = 1$ (Table 3).

To avoid too much switching with graph theory, number theory is covered mainly in the proofs in this section (2.4, 2.6) and in the last section 5, with a few previews in between.

Figure 2: | **Graph transformations yielding the 4-regular middle pages graph G_{MP} (Fig.9)**



2.2 Elementary graph theory

The term *graph theory* dates from the late 19th century, when it was realized that graphs of vertices, points, or nodes connected by edges or arrows to depict family ties, human traffic, molecular structures or serial and parallel electric circuits were mathematical structures in their own right [32]. The definition of a *regular graph* used here (Def.1.2) comes from the very first article by Julius Petersen [33] from 1891 with in its title the word 'graph' as a noun. Consequently, we may also clarify transformed Collatz graphs with well-known graph patterns observed in family trees, hereditary succession, genealogy trees, stars, ladders, bus rides, road maps, Turing tapes, DNA, electric circuits, and communication networks.

The article renowned as the first graph theoretical article [32] is the 1736 article by Leonhard Euler (1707-1783) on a *walk* over the seven bridges of Königsberg [34]. It states that the analysis of sites ("analysis situs") proposed by Gottfried Wilhelm Leibniz (1646-1716) is required to answer the question whether the seven bridges between the four city districts of Königsberg allow for a walk in which each bridge is passed exactly once. A tour, or round trip, in which each bridge, or arrow, is passed once and only once has become known as an *Eulerian tour*. A city quarter with an odd numbers of bridges prevents an Eulerian tour, since finally leaving it requires crossing an already used bridge. The worst prospect for an Eulerian tour is offered by the 3-regular Cayley graph (Fig.1b) in which each node has an odd number of three arrows, one incoming parent arrow and two outgoing arrows to the upward and leftward child.

The 3-regular Cayley graph can be transformed to the 4-regular graph *middle pages graph* (Fig. 9) that allows each branching number a Eulerian round tour, in line with 3-regular-to-4-regular transformations by classic scholars. Plato (427-347bC) knew that each 3-regular cube with three arrows at each node defines a dual 4-regular octahedron with four arrows at each node (Fig.3a). René Descartes (1596-1650) knew that packaging an infinite number of cubes with three lines at each of their nodes gives a 3-dimensional 6-regular coordinate system of adjacent cubes (Fig.3b). This 6-regular coordinate system can be studied however as a projection to a 4-regular coordinate system of adjacent squares, which resembles the 4-regular middle pages graph (Fig. 9).

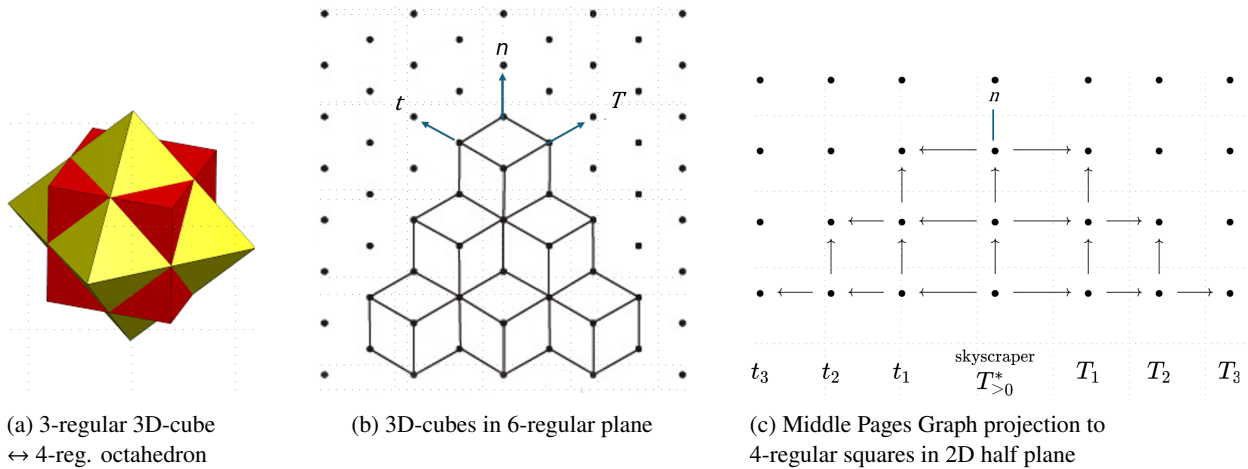


Figure 3: From the 3-regular Cayley graph to the 4-regular Middle Pages graph

Awareness of *breadth-first* ordered (Def. 2.1) and *depth first* ordered (Def.2.2) series in the Cayley graph is required to see that a transformation to a 4-regular graph (Fig.9), similar to the transformation to Fig.3c, can also be applied to the 3-regular Cayley graph (Fig.1b). The 4-regular middle pages graph (Fig.9) allows for Eulerian tours of (infinite congruence classes of) all branching numbers. This enables a proof of the decidability of $an + b$ conjectures (Col.5.14) and a proof of the Collatz conjecture (Col.5.12). The

intermediate transformations required, which are shown in Fig.2, will be detailed in the next sections.

Definition 2.1. *Breadth first order.* The breadth-first order of root paths to nodes in a directed rooted graph is the order by which brothers/sisters, nephews and nieces, grandnephews and grandnieces, and so on, to which no direct successor arrow exists, are visited in a left-to-right order, before own children are visited [35]. Breadth-first ordering an infinite binary tree with a cyclic root gives for breadth-first levels $k = 1, 2, 3, \dots$ a total of 2^k breadth-first ordered root paths to nodes, of which 2 at level $k = 1$ and 2^{k-1} at the highest considered level k .

Definition 2.2. *Depth first order.* The depth-first order of a node to its successors in a directed rooted graph is the order by which children via a direct parent arrow, grandchildren via an indirect grandparent-arrow, great-grandchildren, etc. are visited before brothers/sisters, nephews-nieces, grandnephews-grandnieces etc. are visited to which no such arrows exist [36]. From the point of view of a V-graph foot number, the depth first order by which grandchildren, great-grandchildren, etc. on its V-arms can be visited is already indicated in the Cayley graph (Fig.1b) by the leftward generation s_1, s_2, s_3, \dots or upward generation S_1, S_2, S_3, \dots to which they belong.

A close look at the Cayley tree to be transformed (Fig.1b) shows a collection of V-shaped graphs. Each number in it is both a V-graph foot number and a V-graph arms number, as is highlighted for the number 40 in Fig.6. Each V-arms number can be reached from the trivial root by taking first the breadth-first route to its V-foot number and next the depth-first path from its V-foot number to itself. Each V-arm number can take a different route back to the trivial root. It take a walk to one number of its own generation on either the greedy branch or upward trunk, which have direct connections back to the trivial root. This Eulerian round trip can be already exemplified with Fig.1b for the V-arms number 454 with V-foot number 256 from generation s_2 with as greedy branch number in it 52.

First, the binary number line is extracted by a binary recoding in their breadth-first order of red leftward arrows (red leftward function $L \rightarrow 0$) and of blue upward arrows (blue upward function $U \rightarrow 1$) in the root paths. The skyscraper tape consists of the binary codings of the breadth-first ordered root paths connected to the end numbers of each of these root paths (Fig.5b). This skyscraper tape is put in the gutter of the middle pages graph. For example, V-graph number 256 with binary root path number $UU \rightarrow 11$ becomes the number pair $\frac{11}{256}$ in the skyscraper tape in the gutter of the middle pages graph starting from the trivial root number pair $\frac{0}{4}$.

$$\text{Skyscraper tape} \quad \begin{array}{l} \text{left, binary number line} \\ \text{right, root path end numbers} \end{array} \quad \begin{array}{l} 0, 1; \\ 4, 16; \end{array} \quad \begin{array}{l} 10, 1; \\ 40, 256; \end{array} \quad \begin{array}{l} 100, 101, 110, 111; \\ 52, 160, 340, 1024; \end{array} \quad \begin{array}{l} 1000, \dots \\ 34, \dots \end{array} \quad (2.1)$$

Second, the depth-first order by which V-foot number number pair $\frac{11}{256}$ can walk to its leftward successor pair $\frac{11100}{454}$ in leftward generation s_2 on its V-arm numbers (Fig.1b) is put in the row to the right of $\frac{11}{256}$ (Fig.9).

Third, the number pair $\frac{11100}{454}$ in generation s_2 is considered as a breadth-first-ordered number in its own cotree t_2 (Fig.7d) connected to the t_2 cotree root number 52, which is located in the 3-regular Cayley graph on the greedy branch. Thus, the 3-regular Cayley graph (Fig.1b) allows already to see that $\frac{11100}{454}$ can reach $\frac{100}{52}$ as the root number from its own generation s_2 on the greedy branch.

Fourth, the greedy branch root number $\frac{100}{52}$ can return to the trivial root number pair $\frac{0}{4}$ since the greedy branch and the upward trunk are defined as paths connecting their numbers to the trivial root (Defs.3.9,3.10).

Periodic density of binary numbers coding breadth-first ordered root paths

The binary number line of successively coded breadth-first root paths a carries the wondrously ordered numbers x with it in the skyscraper tape (Eq.2.1). Tapes of $\frac{a}{x}$ number pairs are associated with a *Turing*

tape of binary memory addresses a pointing to interesting program steps x in the memory cells [12]. The skyscraper tape resembles even more the mechanical *calculus ratiocinator* designed and partly build by Gottfried Wilhelm Leibniz (1646-1716) in which decimal numbers x only serve as inputs and outputs, while pointing to binary numbers a for interesting and fast calculation [37, ch.4.2].

Corollary 2.3. *The skyscraper graph representing an $an + b$ function does not resort to the encoding of non-numerical “words” or “node labels” to distinguish the nodes.* The distinctions between the nodes in a non-regular binary graph without a cyclic root resorts to non-numerical “words” or “node labels” [38, 39, 40], and so do decidability approaches using the (occurrence of specific letters) in “words” [41]. However, in the skyscraper graph (Fig.5b) the 3-regular Cayley colour graph (Fig.1b) of an $an + b$ function connected to $c = a + b$, nodes can be specified as number pairs $\frac{a}{x}$, in which a is a binary number representing the breadth-first order of a root path and x is the number to which the root path is pointing. \square

The calculations below with the binary number line in the left string of the skyscraper tape deal with the periodic density of number pairs in the columns of the middle pages graph (Col.2.4). Next they enable fast checks of convergence to the trivial root for arbitrary numbers (Col.2.6), given the proof of the Collatz conjecture, which implies for arbitrary $k \in 1, 2, 3, \dots$ a proof on 2^k breadth-first ordered numbers in the Cayley color graph. These breadth-first ordered numbers are spread over the depth-first ordered leftward generations s_1, s_2, s_3, \dots and over the depth-first ordered upward generations S_1, S_2, S_3, \dots (Fig. 1b, Col.2.4, 5.12)). In the 3-regular Cayley graph (Fig.1b) each branching number is both the V-foot number of a V-shaped graph and a V-arms number in a different V-shaped graph. In its transformation to the 4-regular middle pages graph (Fig.9) each number pair occurs both as a V-foot number pair in the its gutter and as a V-arms number pair in its rows.

Corollary 2.4. *The cumulative periodic density of odd and even binary numbers as first numbers in leftward and upward number pairs on V-graph arms in the rows of the middle pages graph (Fig.9) is 1.* The binary number line of successively coded breadth-first root paths a carry the wondrously ordered numbers x with them in the number pairs of the skyscraper tape (2.1) in the gutter of the 4-regular middle pages graph (Fig.9). In the 3-regular Cayley graph each branching number is the V-arm number of a V-graph (Figs.1b,6). Each V-foot number spreads its V-arms, which become rows in the middle pages graph, such that each number pair on the V-arms in the rows of the middle pages graph is the successor of a V-foot number pair in the gutter of the middle pages graph, and all number pairs in V-arms in the rows are also number pairs in V-foots in the gutter of the middle pages graph. Numbers on V-arms in the rows of the middle pages graph come from the disjoint leftward generations s_1, s_2, s_3, \dots (Def.3.11, Fig. 1b) and disjoint upward generations S_1, S_2, S_3, \dots (Def.3.12, Fig. 1b). Numbers in these generations are now the numbers in the columns of the left page and the right page of the middle pages graph. Leftward number pairs s_1, s_2, s_3, \dots on the left page of the middle pages graph have *even* binary numbers as first numbers with a periodic density of $1/2$. Number pairs on the right page have *odd* binary numbers as first numbers also with a periodic density of $1/2$. These periodic densities of $1/2$ are divided in a geometric series over successive leftward generations $\frac{s_1}{1/4}, \frac{s_2}{1/8}, \frac{s_3}{1/16}, \dots$ and successive upward generations $\frac{S_1}{1/4}, \frac{S_2}{1/8}, \frac{S_3}{1/16}, \dots$. A few of these column densities are shown in a top row of the middle pages graph (Fig.9). \square

The remaining question is whether the binary numbers a in number pairs $\frac{a}{x}$ in the Collatz graph carry all the branching numbers x delivered by Collatz’s $3n + 1$ function with them. The proof is that the Collatz function enables for all branching numbers a Eulerian round trip to and from the trivial root number pair $\frac{0}{c=a+b=4}$ in the middle pages graph (Fig.9) such that the density of branching numbers x as second numbers in number pairs $\frac{a}{x}$ in the columns on the left page and the right page of the middle pages graph equals the density of all branching numbers (Col.5.12). It is easy to prove that all non-branching numbers can walk to branching numbers (Def.5.5).

Only a fraction of the root paths generated by $an + b$ functions that fail for the decidability test 1.4, such as $5n + 1$ and $3n - 1$ (Table3), are connected to the trivial root $c = a + b$ and included in the skyscraper tape

with $\overset{0}{c=a+b}$ as lowest number pair. The skyscraper tape of an $an + b$ function failing for the decidability test still includes on its left stander the countably infinite set of all binary numbers $0, 1; 10, 11; 100, \dots$ with a periodic density of 1 (2.4). The memory cells to which these binary numbers point belong however to the *subset* of branching numbers generated by the function $an + b$ located at the end nodes of root paths connected to $c = a + b$.

Corollary 2.5. *Periodic density test whether an $an+b$ function converges only to $c = a+b$.* The decidability test whether an $an + b$ function lets all natural numbers converge to the trivial root $c = a + b$ (Theorem 1.4) can be verified with calculations whether the periodic density of all numbers in the skyscraper graph (Eq.2.1, Fig.5b) pointed to by binary numbers representing breadth-first ordered root paths (which have themselves a density of 1 (Col.2.4)) equals the periodic density of all branching numbers generated by the $an + b$ function. The skyscraper graph is the fold of the middle pages graph, thus this test can be performed on cotree skyscraper columns on the left and right page of the middle pages graph (Fig.9). \square

Corollary 5.12 proves that the Collatz function $3n + 1$ passes this density test.

A proof of the Collatz conjecture enables fast checks

The $P = NP$ Clay millennium problem raised by computer scientist Stephen Cook is whether all problems with growing difficulty k whose solution can be *checked* with a polynomial increase of resources $P = k^a$ (often $a = 2$ or $a = 3$), or even with less than a linear increase of resources $P < k$, can also be *proven* with a polynomial increase of resources NP [42]. The proof of the Collatz conjecture reverses the $P = NP$ question to whether a fast check is possible. A proof of the Collatz conjecture would apply to all breadth-first levels $k = 1, 2, 3, \dots$ in an infinite Cayley color graph, which contain an exponentially growing amount of 2^k numbers of which 2^{k-1} at the highest level holding k L and U arrows ($k = 5$ for Fig.1b, $k = 18$ for Fig.4). Assuming this proof, the heuristic term rewriting approach [15, 14] can be turned into a very fast method to check the convergence of one of these 2^{k-1} numbers in linear time k , and for all but one number in less than linear time k 2.6. 1

Corollary 2.6. *For all but one of the 2^{k-1} highest level numbers in breadth-first level k convergence to the trivial root can be checked in less than k steps.* Since numbers in the columns of the left page and right page of the middle pages graph can be reached in parallel, checking whether a number has a root path to the trivial root (Fig.9) requires no computation for each separate number in a root path, but a computation for each of the cotree columns over which a root path is spread, which is the number of switches between 0 (red) and 1 (blue) in the binary representation of the root path in the skyscraper graph. Thus, the number of steps in the fast check using the term rewriting approach [15] is the number of cotree switches (1). \square

The convergence to the trivial root can be checked in less than $k = 5$ steps for all $2^{5-1} = 16$ numbers on the highest level in Fig.1b except for 1696 with alternating blue upward and red leftward arrows in its root path $4 \rightarrow 16 \rightarrow 40 \rightarrow 160 \rightarrow 106 \rightarrow 1696$. Check 2.6 shows in $k = 1$ step the convergence to the trivial root of the example number 454 above, which was one out of $2^{5-1} = 16$ branching numbers at level 5 in Fig.1b. Only cotree t_2 with root $\overset{100}{52}$ on the greedy branch is involved in the check. Just 8 steps of cotree switches suffice to check the convergence of the example number 31 from the term rewriting literature [15] having $3n + 1$ image 94. 94 holds one out of 2^{42-1} root paths with length 42 in the Cayley oolour graph (Table 1).

3 Transformations of the Collatz graph G_C and the 3-regular Cayley colour graph $T_{\geq 0}$

The Collatz graph G_C , partly depicted in Fig. 1a, is an *infinite directed graph*, specified in Eq. 3.1 as a pair $G = (V, E)$ of a set of vertices or nodes V , and a set of arrows E [4, 27].

$$\begin{aligned} \text{Collatz graph } G_C &= (\omega_0, [f, g]), & \text{in which (Fig. 1a):} & (3.1) \\ \omega_0 &= \{1, 2, 3, \dots\}, & \text{the well-ordered set of natural numbers,} & \\ f: n &\rightarrow (n-1)/3, & g: n &\rightarrow 2n, \\ f^{-1}: n &\rightarrow 3n+1, & g^{-1}: n &\rightarrow n/2 \end{aligned}$$

Its *nodes*, or vertices V , are all numbers n from the infinite set of the well-ordered natural numbers $\omega_0 = 1, 2, 3, \dots$. The arrows in Fig. 1a represent the subfunctions $f: n \rightarrow (n-1)/3$ and $g: n \rightarrow 2n$. Steps $f^{-1}: n \rightarrow 3n+1$ and $g^{-1}: n \rightarrow n/2$ in the reverse direction of arrows f and g are conjectured to let all numbers converge to the trivial root. The uncoloured non-branching numbers in Fig. 1a either have just one child, or two children of which one does not have branching numbers in its offspring. For example, 10 is a non-branching number because its child 3 and its $g: n \rightarrow 2n$ offspring $3 \rightarrow 6 \rightarrow 12 \rightarrow 24 \rightarrow 48 \rightarrow \dots$ are divisible by 3, and therefore unreachable by $3n+1$ and not divisible by 3 after subtraction of 1 (Fig. 1, grey-coloured line graphs).

The Collatz graph G_C (Fig. 1a) is *irregular*, given definition 1.2 of a regular graph [33][4, ch.1.2]. Each number in it has one incoming arrow from its parent (and therefore an indegree of 1), either an f or g arrow. Not all numbers have two children, since $f: n \rightarrow (n-1)/3$ is undefined where it would have given a fraction with (a power of) 3 in its nominator.

Fig. 1b shows the transformation of the lowest part of the irregular Collatz graph in Fig. 1a into the lowest part of a Cayley color graph labeled $T_{\geq 0}$ holding exclusively branching numbers. The Cayley color graph $T_{\geq 0}$ is a 3-regular graph (Def. 1.2). All branching numbers have a parent, including the trivial root number $c = 4$, which is its own parent. All branching numbers have two children, including the trivial root number $c = 4$, which is its own leftward child. The *uncolored* non-branching numbers in Fig. 1a are removed, i.e. transformed to *invisible* numbers.

The Cayley graph $T_{\geq 0}$ is named after Arthur Cayley (1821-1895), the originator of regular color graphs and their graphical representation [43]. To the best of our knowledge, Fig. 1b is the first exemplar of an *infinite* Cayley colour graph. Equation 3.2 below captures a part of its full definition of its nodes and arrows in subsection 5.1.

$$\begin{aligned} \text{Cayley graph } T_{\geq 0} &= (S_{\geq 0}, [L, U]), \text{ in which (Fig. 1b):} & (3.2) \\ S_{\geq 0} &= [4, 16]_{18}, \text{ branching classes, residues 4 or 16 mod 18 (Eq. 5.1)} \\ L: n &\rightarrow fg^i(n), \quad U: n \rightarrow g^j(n), \quad \text{given } i \in 1, 2, 3, 4; j \in 2, 4 \text{ (Defs. 5.1, 5.2),} \end{aligned}$$

The blue and red branching numbers in it are the numbers with either a residue of 4 or 16 after division by 18, denoted as $S_{\geq 0} = [4, 16]_{18}$ (Eq. 5.1). Applying $(n-1)/3$ to them gives the odd congruence classes $[1, 5]_6$ not divisible by 3 (Eq. 5.1), which inhabit the Syracuse tree of odd numbers after the removal of numbers divisible by 3 ([17, Prop. 1.17]). Red and blue paths with uncoloured non-branching numbers in Fig. 1a are in Fig. 1b shortened to red arrows $\xrightarrow{L} = fg^i$ (Def. 5.2) by the leftward function to and blue arrows $\xrightarrow{U} = g^j$ (Def. 5.1) by the upward function. The indices i and j are specified in the definitions of the *upward* function (Def. 5.1) and of the *leftward* functions L (Def. 5.2). Each subclass of the uncoloured non-branching numbers in the Collatz graph (Fig. 1a) allows for a walk to a subclass of branching numbers, as specified by the *forward* function F (Def. 5.5, Lemma 5.6).

3.1 The planar Cayley graph as an infinitely dimensional fractal binary tree

The Collatz graph $T_{\geq 0}$, which is analytically shown as a planar graph with 5 breadth-first levels in Fig. 1a, can be depicted more intuitively as an infinitely dimensional fractal binary tree T_{CF} (Fig. 4), here with 18 breadth-first levels, giving $2^{18} = 262144$ root paths that cannot be visually distinguished anymore. It still does not include the root paths with more than 18 arrows of 9 out of 32 branching numbers lower than 288, namely those of 94, 124, 142, 166, 214, 220, 250, 274 and 286. The height of numbers reflects however their true number size. Fractal trees were introduced by Benoit Mandelbrot (1924-2010) [44].

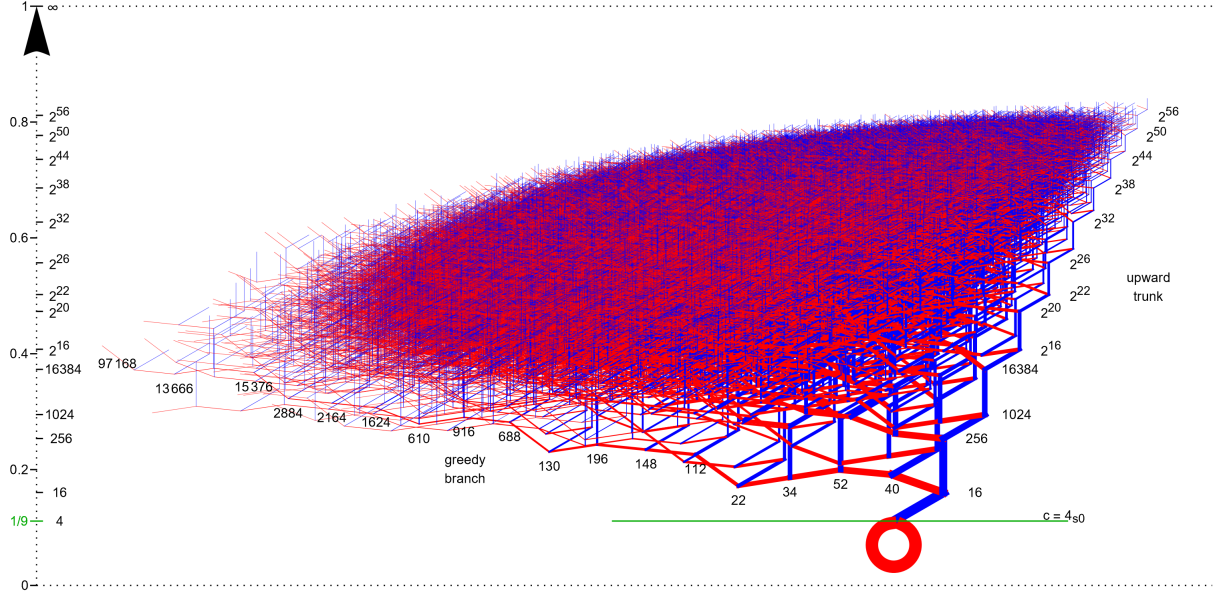
The fractal graph depicts the wondrously ordered Collatz numbers according to their magnitude, or height. The lengths and angles of the arrows of a fractal tree are also referred to as the *magnitudes* and *directions* of its vectors in a metric vector space. Lengths of arrows, or magnitudes of vectors, are also referred to as the *distances* between the start nodes and the end nodes of arrows.

The *lengths* of the arrows, and for aesthetic reasons also the width of the arrows, contract further at each breadth-first level k to $m_k = a(1-a)^{k-1}$, for $k = 1, 2, 3, \dots$, in which a is chosen as $1/3^2$. The cumulative length of the arrows at levels $k = 1, 2, 3, \dots$ comes arbitrarily close to the horizon 1 of the open interval $(0,1)$, since the limit of the geometric series sum $s = \sum_{k=1}^{\infty} a(1-a)^{k-1}$ amounts to $s = a/(1-r) = a/(1-(1-a)/a) = 1$. Were the number of breadth-first iterations to be increased further (Fig. 4, $k = 18$, thus only $2^k = 262144$ root paths), then the crown of the depicted part of the fractal tree would become flatter and flatter. Without contraction at each successive breadth-first level (by $8/9$), the crown of the tree would become increasingly sloping, even on a logarithmic scale.

Remark 3.1. *Optical illusions due to the hyperdimensionality of fractal tree T_{CF} .* The fractal tree offers an intuitive depiction of the Collatz graph, but also optical illusions. The crossings of straight branches where one arrow appears to fork in three or more arrows instead of two arrows may suggest that these crossings would disappear if the arrows could be seen in three dimensions. It is however impossible to place them in front of each other while preserving all lengths and all angles of arrows. Removing the crossings that are not nodes while preserving the lengths and angles of successive vectors without cutting or stretching them requires an *infinitely dimensional metric vector space*, also labelled a *hyperdimensional space*. Because cutting or stretching them would be required, the fractal tree (Fig. 4) is *not homeomorphic* to the planar tree (Fig. 1b) unless *root-homeomorphism* would be accepted, meaning that each number in the fractal binary tree can be absorbed by its cyclic root and be reproduced thereafter in a planar tree. \square

Remark 3.2. *Anti-symmetric fractal Collatz cotrees without same-angle arrows.* The legend to Fig. 4 highlights that all leftward vectors in the fractal Collatz graph are *anti-symmetric* because they have different angles (converging to only 4 angles). Anti-symmetry is known in physics from Enrico Pauli's (1901-1954) exclusion principle and Paul Dirac's (1902-1984) anti-symmetric ladder operator. All arrows in the first leftward and upward cotree (cotrees t_1 and T_1 , Figs. 7b and 8b) have different angles, yielding entirely anti-symmetric fractal cotrees. The node numbers in cotrees t_1 and T_1 come from $72 + 81 = 153$ congruence classes modulo 32 gross $= 288 \cdot 2^4 = 4608$ (Table 2, node sets $[c72]_{288 \cdot 2^4}$ and $[c81]_{288 \cdot 2^4}$). The number 153, associated with the number of fish in the miraculous fish catch (John:21), is the number of arrows, or edges, in the *symmetric, distance-regular*, Biggs-Smith graph [4]. \square

Figure 4: The Cayley graph $T_{\geq 0}$ as the infinitely dimensional fractal binary tree T_{CF}



Legend |. The lowest Collatz numbers 4, 16, 22, 34, 40, 52, ... that will be encountered in the breadth-first, left-to-right traversal of tree $T_{\geq 0}$ are paired with the binary numbers representing their breadth-first ordered Collatz root paths. They have the lowest projections to the vertical axis of the fractal tree T_{CF} .

$$T_{\geq 0} : \quad \begin{array}{ccccc} 0 & , & 1 & , & 10000 & , & 1000 & , & 10 & , & 100 & , & \dots \end{array} \quad (3.3)$$

$$T_{CF} : \quad \begin{array}{ccccc} 0 & , & 1 & , & 10000 & , & 1000 & , & 10 & , & 100 & , & \dots \end{array} \quad (3.4)$$

The *angles* of the arrows represent the expansion or contraction of children relative to their parents. Upward arrows $U : n \rightarrow n \cdot 2^4$ with arguments from class $[16]_{18}$ give a maximum expansion of parent numbers by a factor 4 on a logarithmic scale with base 2 (Def:5.1). Upward arrows $U : n \rightarrow n \cdot 2^2$ with arguments from class $[4]_{16}$, which expand parent numbers halve as much on a logarithmic scale, therefore obtain a diagonal angle of $\alpha_n = 1/4\pi(45^\circ, \text{e.g. } 4 \rightarrow 16)$. Leftward iterations $n \rightarrow (n-1)/3 \cdot 2^q$ give infinitely many different angles, which come arbitrarily close to four angles $1 - 1/8 \log_2(2^q/3))\pi$, for $q = 1, 2, 3, 4$ (Def.2). These asymptotic angles amount to a contracting angle of approximately $\alpha_n \approx 1.073\pi \approx 193^\circ$ (or $\approx -17^\circ$) for $q = 1$, and to three expanding angles of approximately $\alpha_n \approx 0.948\pi \approx 170.7^\circ$ for $q = 2$, $\alpha_n \approx 0.875\pi \approx 158^\circ$ for $q = 3$, and $\alpha_n \approx 0.823\pi \approx 148^\circ$ for $q = 4$. For example, the angle α_{40} of the arrow $L : 40 \rightarrow 52$, for which $q = 2$ (Def.2) is $\alpha_{40} = 1 - 1/8 \log_2((40-1)/3 \cdot 2^2/40))\pi$, which is approximately $\alpha_{40} \approx 0.953\pi \approx 171.5^\circ$.

The vectors with length m_k and angle α_n from parent numbers to child numbers, in combination with their projections to vertical line segments with length $m_k \sin \alpha_{n(k)}$ on the vertical axis makes it possible to use Pythagoras to compute also the horizontal projections. The vertical length of the projection of each root path to the vertical axis consists therefore of successive line segments $m_k \sin \alpha_{n(k)}$, as shown above (Fig.3.4) for the number pairs with the lowest Collatz numbers 4, 16, 22, 34, 40 and 52. |

3.2 Transforming Jacob's ladder (Fig. 5a) to its dual skyscraper tape (Fig. 5b)

Jacob's infinite ladder to heaven (Fig. 5a), known from Jacob's dreams in the book of Genesis and artist impressions thereof, becomes via a serial-to-parallel transformation the skyscraper tape (Fig. 5b), which is draped in the gutter of the 4-regular middle pages graph (Fig. 9). Jacob's ladder and its skyscraper tape resemble Turing's tape [12], with as their left stander the binary number line. Binary coded root paths a carry wondrously ordered numbers x with them that are connected to the trivial root.

Coding the colours of arrows in the breadth-first *zigzag* order of successive root paths (Def. 2.1, $L \rightarrow 0, U \rightarrow 1$ for L, U ; UL, UU ; ULL, \dots) to successive branching numbers 4, 16; 40, 256; 52, \dots to a *linear* order transforms the Cayley graph (Fig. 1b) to Jacob's ladder graph (Fig. 5a). Root paths on the rungs of Jacob's ladder to numbers consist of L and U arrows to them (Fig. 1b), of which L is coded as 0 and U is coded as 1 on the left stander of the ladder. Its left stander are successive binary numbers on the binary number line coding successive breadth-first ordered root paths on the rungs of Jacob's ladder.

$$\text{Jacob's ladder} \begin{array}{l} \text{left, binary number line} \\ \text{rungs, root paths (breadth-first)} \end{array} \begin{array}{l} 0, 1; \\ L, U; \end{array} \begin{array}{l} 10, 11; \\ UL, UU; \end{array} \begin{array}{l} 100, 101, 110, 111; \\ ULL, ULU, UUL, UUU; \end{array} \begin{array}{l} 1000, \dots \\ ULLL, \dots \end{array} \quad (3.5)$$

The breadth-first ordered root paths lead to successive Collatz output numbers 4, 16; 40, 256; 52, \dots in their wondrous order.

$$\text{Jacob's ladder} \begin{array}{l} \text{rungs, root paths (breadth-first)} \\ \text{right, root path end numbers} \end{array} \begin{array}{l} L, U; \\ 4, 16; \end{array} \begin{array}{l} UL, UU; \\ 40, 256; \end{array} \begin{array}{l} ULL, ULU, UUL, UUU; \\ 52, 160, 340, 1024; \end{array} \begin{array}{l} ULLL, \dots \\ 34, \dots \end{array} \quad (3.6)$$

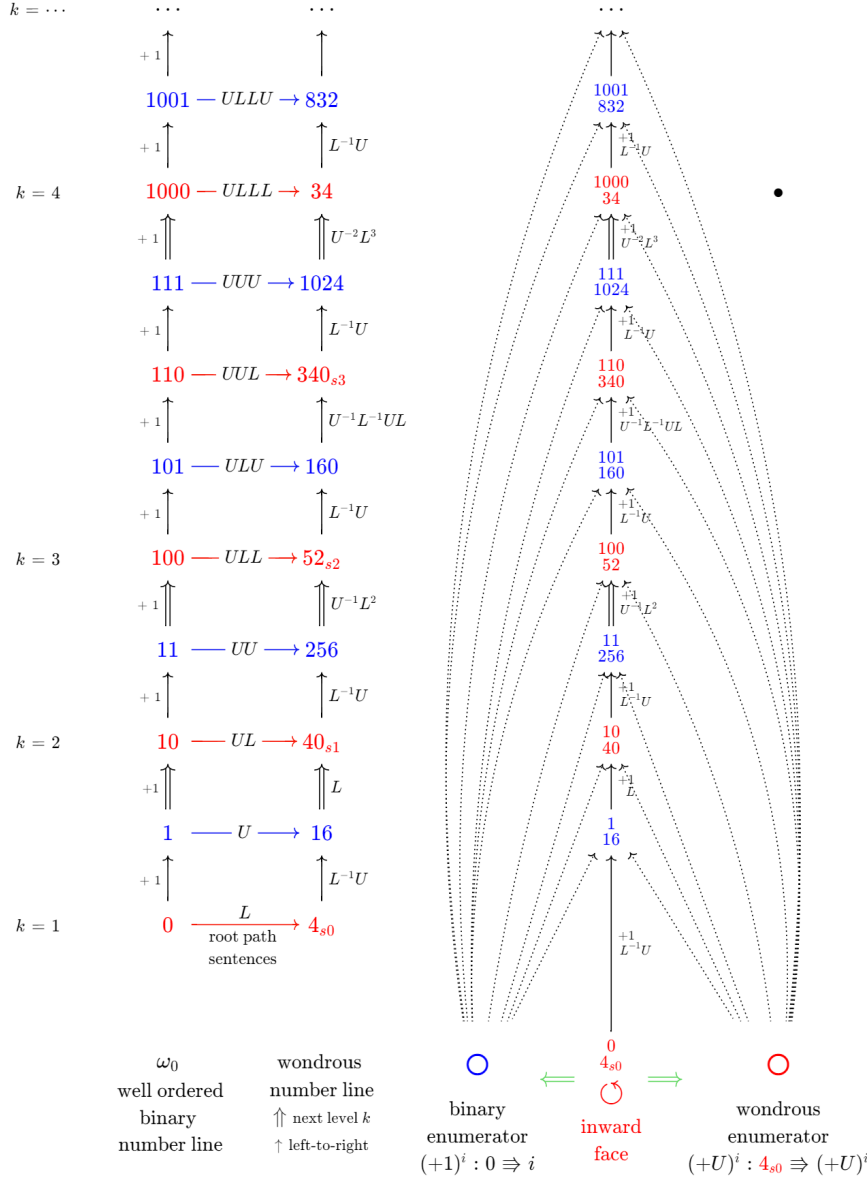
The transformation to a Turing tape [12] of paired binary memory cell addresses on the left stander pointing to memory cells holding end numbers of root paths on the right stander of Jacob's ladder is the serial-to-parallel transformation to a *dual graph*. The transformation to a dual graph is well-documented for undirected finite graphs (Def. 3.3). This dual graph is a Turing tape, labeled here as the *skyscraper tape*, depicted already (Eq. 2.1). It becomes the gutter, or fold, or middle column, of the 4-regular middle pages graph (Fig. 9).

Definition 3.3. *Transformation to a dual graph of an undirected finite graph.* Given a finite planar graph G , its geometric dual G^* is constructed by placing a vertex/node in each region/site/face of G (including the exterior region/site/face) and, if two regions/sites/faces have an edge x in common, joining the corresponding vertices/nodes by an edge X^* crossing only x .

The formation of a dual graph from a directed infinite graph (Def. 3.4) uses that the countably infinite number of sites reached in parallel can be named after the end numbers of the serially connected arrows crossed.

Definition 3.4. *Transformation to a dual graph of a directed infinite number graph.* Given a infinite planar graph G with nodes named/labeled by the natural numbers (e.g. 0, 1; 10, 11; 100, \dots or 4, 16; 40, 256; 52, \dots) or other labels, its geometric dual G^* is constructed by placing a vertex/node in each region/site/face of G (including the exterior regions/sites/faces) and, if two sites/faces are separated by an arrow x , connecting the vertices/nodes separated by x by an arrow X^* crossing only x , while naming/labeling the site/face that becomes the end node of X^* after crossing x with (the natural number or label identifying the) the end node of x . None of the arrows of a node towards one of its children is considered as an arrow x that separates external sites.

Figure 5: Jacob's ladder and its dual skyscraper graph in the fold of the middle pages graph G_{MP}



Legend | a. Based on the Cayley graph (Fig.1b), the rungs of Jacob's ladder are successive breadth first-ordered root paths $L, U; UL, UU; ULL, \dots$. The coding slider of Jacob's ladder codes these breadth-first ordered root paths by $L \rightarrow 0$ and $U \rightarrow 1$ as successive binary numbers $0, 1; 10, 11; 100, \dots$ with binary steps of $+1$. The complementary slider consists of successive Collatz root path outputs $4, 16; 40, 256; 52, \dots$ in a wondrous order **b.** The infinite breadth-first Collatz tape consists of a countably infinite number of paired binary addresses of root paths and Collatz root path outputs $\frac{0}{4}, \frac{1}{16}, \frac{10}{40}, \frac{11}{256}, \frac{100}{52}, \dots$. Next to numbers the nodes of the skyscraper tape comprise enumerators of binary numbers and wondrous numbers that are exponential functions that in parallel generate (additive) exponents: all binary addresses are for example generated in parallel by the binary enumerator $(+1)^i : 0 \rightarrow i$, for $i = 1, 2, 3, \dots$ ([45, 6.021]) |

Jacob's ladder offers 3 additional footholds, or 'sites', or 'faces', to put a step, beyond the totality of its rungs coded by the totality of binary numbers: downstairs below rung 1, to the left of the ladder, and to the right of the ladder. These 3 additional footholds, or sites, or faces, become by the serial-to-parallel transformation (Def, 3.4) the bottom nodes in the dual skyscraper graph (Fig.5b) and consequently in the dual middle pages graph (Fig.9) from which serially connected nodes can be reached in parallel. They do not become numbers, but naming functions, or enumerator functions of an exponential nature [45, 6.021].

The ladder graph overcomes the apparent self-referentiality of the Collatz function. In his book *Escher, Gödel, Bach* Douglas Hofstadter's character Achilles rated this "wondrousness problem" as "wondrous tricky" [2, p402]. Hofstadter discusses examples of self-referential theories and statements that were shown to be undecidable because of their self-referentiality. The Collatz subfunctions f^{-1} and g^{-1} in the irregular Collatz graph (Fig.1a) appear to be self-referential. They map each natural number *injectively* to a wondrous path of subfunctions f^{-1} and g^{-1} to a root number, conjectured to be always 1. Since $f : n \rightarrow (n - 1)/3$ may yield a fraction, not all combinations of these subfunctions yield natural numbers.

Corollary 3.5. *The rungs of Jacob's ladder, and the number pairs in the skyscraper tape, are arguments and outputs of a not self-referential function. Each number pair $\frac{a}{x}$ in the skyscraper tape is a numerical $a \rightarrow b$ function. It specifies a binary number argument a representing successive L and U arrows in the root path of a number to the wondrous number x generated by these successive L and U arrows in the root path. This is a *not self-referential number function* with numeric arguments a and numeric outputs x . □*

3.3 Transforming the duals of depth-first ordered V-arms (Fig.6) to rows in the middle pages graph

The *depth-first* order can be seen in the 3-regular Cayley graph (Fig.1b) from the partition of nodes in successive leftward generations s_1, s_2, s_3, \dots and successive upward generations S_1, S_2, S_3, \dots . These successive generations build the rows in the 4-regular middle pages graph (Fig.9), paired in Turing tapes to their breadth-first addresses (Fig.6). Each branching number is both the foot number of its own V-graph and a V-arm number in a different V-graph with a different V-foot number.

Each branching number is as a V-foot number serially connected to leftward V-arm numbers in each of the leftward generations s_i through the composite function UL^i for $i = 1, 2, 3, \dots$ (Eq.3.11, examples 3.7,3.9). Each branching number is as a V-foot number also serially connected to upward V-arm numbers in each of the upward generations S_j through the composite function LU^j for $j = 1, 2, 3, \dots$ (Eq.3.12, examples 3.8,3.10). Here we use the *diagrammatic notation* [46, p.33], or *leftmost innermost-notation* [47, p.906] for composite functions such as UL^i . This separates functions from their inputs and outputs, or authors from their statements, by a colon. The leftmost-innermost order is for example also the order of matrices in matrix algebra.

The numbers in the rows on the middle pages middle pages graph (Fig.9), are simply obtained by flattening the *depth-first* trajectories from V-foot numbers to V-arms numbers (Fig.6) belonging to leftward generations s_1, s_3, s_3, \dots or upward generations S_1, S_2, S_3, \dots . The examples 3.7 and 3.8 deliver the first numbers on the second lowest number row in the 4-regular middle pages graph (Fig.9). The examples 3.9 and 3.10 deliver the first numbers of the greedy branch and the upward trunk on the lowest number row of the middle pages graph (Fig.9, compare Fig.1b).

$$\text{V-foot 40's leftward arm:} \quad UL^{i=1,2,3,\dots} : \frac{10}{40} \rightarrow \frac{1010}{106_{s1}} \rightarrow \frac{10100}{70_{s2}} \rightarrow \frac{101000}{368_{s3}} \rightarrow \dots \quad (3.7)$$

$$\text{V-foot 40's upward arm:} \quad LU^{j=1,2,3,\dots} : \frac{10}{40} \rightarrow \frac{1001}{832_{S1}} \rightarrow \frac{10011}{3328_{S2}} \rightarrow \frac{100111}{53248_{S3}} \rightarrow \dots \quad (3.8)$$

$$\text{Greedy branch, 4's leftward arm:} \quad UL^{i=1,2,3,\dots} : \frac{0}{4_c} \rightarrow \frac{10}{40_{s1}} \rightarrow \frac{100}{52_{s2}} \rightarrow \frac{1000}{34_{s3}} \rightarrow \frac{10000}{22_{s4}} \rightarrow \dots \quad (3.9)$$

$$\text{Upward trunk, 4's upward arm:} \quad LU^{j=1,2,3,\dots} : \frac{0}{4_c} \rightarrow \frac{1}{16_{S1}} \rightarrow \frac{11}{256_{S2}} \rightarrow \frac{111}{1024_{S3}} \rightarrow \dots \quad (3.10)$$

$$\text{Leftward generations, cosets:} \quad UL^{i=1,2,3,\dots} : S_{\geq 0} \rightarrow s_1 \rightarrow s_2 \rightarrow s_3 \rightarrow \dots \quad (3.11)$$

$$\text{Upward generations, cosets:} \quad LU^{j=1,2,3,\dots} : S_{\geq 0} \rightarrow S_1 \rightarrow S_2 \rightarrow S_3 \rightarrow \dots \quad (3.12)$$

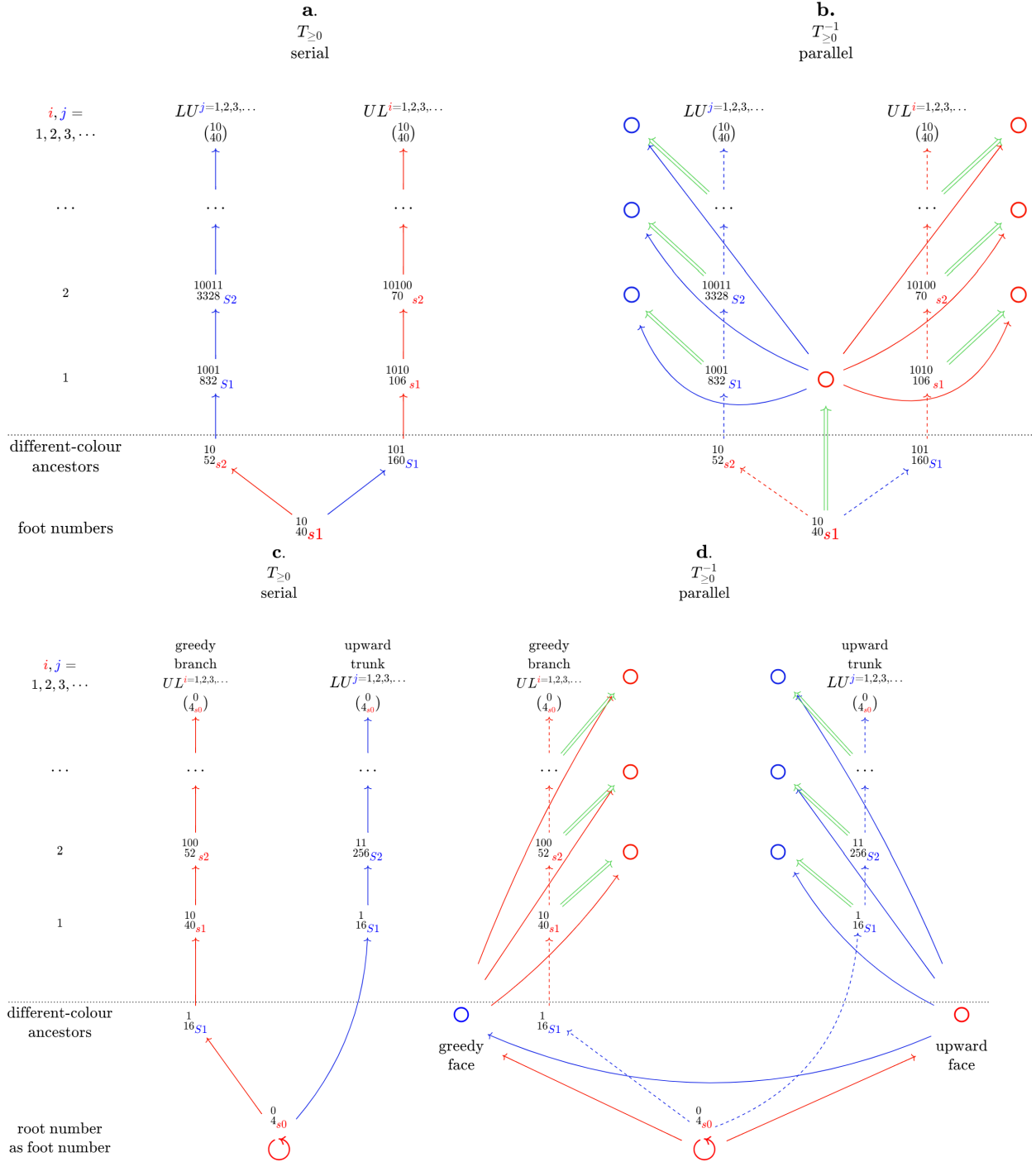
$$\text{Leftward cotrees (Fig.7bdf):} \quad UL^{i=1,2,3,\dots} : T_{\geq 0} \rightarrow t_1 \rightarrow t_2 \rightarrow t_3 \rightarrow \dots \quad (3.13)$$

$$\text{Upward cotrees (Fig.8bdf):} \quad LU^{j=1,2,3,\dots} : T_{\geq 0} \rightarrow T_1 \rightarrow T_2 \rightarrow T_3 \rightarrow \dots \quad (3.14)$$

$$\text{Leftward subtrees (Fig.7ace):} \quad L^{i=1,2,3,\dots} : T_{\geq 0} \rightarrow t_{\geq 1} \rightarrow t_{\geq 2} \rightarrow t_{\geq 3} \rightarrow \dots \quad (3.15)$$

$$\text{Upward subtrees (Fig.8ace):} \quad U^{j=1,2,3,\dots} : T_{\geq 0} \rightarrow T_{\geq 1} \rightarrow T_{\geq 2} \rightarrow T_{\geq 3} \rightarrow \dots \quad (3.16)$$

Figure 6: Serial V-arms in-parallel flattened to rows in the 4-regular Middle pages graph (Eqs.3.7-3.10)



Legend |. $\begin{pmatrix} 10 \\ 40 \end{pmatrix}$ is the V-foot number pair in V-graph **c**, and a V-arm number pair in **a**. The root $\begin{pmatrix} 0 \\ 40 \end{pmatrix}$ is also a V-foot number pair because it is its own child. It is not a V-arm number. The dual graphs **b** and **d** are obtained by naming sites, or faces after the number pairs at the end nodes of arrows crossed to reach them from the other side of these arrows.

3.4 From tree $T_{\geq 0}$ to skyscraper tapes of isomorphic cotrees (Defs.3.13,3.14, Figs.7,8)

All numbers in successive leftward generations s_1, s_2, s_3, \dots and upward generations S_1, S_2, S_3, \dots build the successive columns on the left page, respectively the right page, of the the 4-regular middle pages graph (Fig.9). These columns are cotree skyscraper tapes of the breadth-first ordered numbers in cotrees t_1, t_2, t_3, \dots (Fig.7bdf) and T_1, T_2, T_3, \dots (Fig.8bdf). Cotrees are obtained by applying the functions UL^i and LU^j , for $i, j = 1, 2, 3, \dots$ not only to the numbers (Eq.3.11, 3.12) of the Cayley graph $T_{\geq 0}$, but also to its arrows (Eq. 3.13, 3.14). The numbers on the lowest row of the cotree skyscraper tapes are successive numbers on the greedy branch, repectively the upward trunk (Fig.1b).

The Cayley color graph (Fig.1b), its leftward and upward cotrees (Figs.7bdf, 8bdf) generated by the functions 3.13 and 3.14, and its subtrees (Figs.7ace, 8ace) generated by the functions 3.15 and 3.16 are all *isomorphic* to each other. Informally, two rooted infinite planar graphs are isomorphic if their nodes are connected in the same way [48], implying that they can be picked up by their roots after which their arrows can be stretched in such a way that both of them can be put on top of the other such that all nodes and arrows in the other are covered. Two graphs are isomorphic to each other if the *transformation function* $w^{-1}vw$ (Def.3.6.Eq. 3.17) applies, which was introduced by Max Dehn (1878-1952) in 1911 [7].

Definition 3.6. Isomorphic graphs. Two graphs G and H are isomorphic if all start nodes m and end nodes n of each arrow v in graph G may complete a collective walk w to their respective output nodes $w(m)$ and $w(n)$ in graph H . This collective walk w implies the possibility of an indirect walk $w^{-1}vw$ from $w(m)$ to $w(n)$, on the basis of which the transformation function generates a *conjugate inner arrow* $v_1 = w^{-1}vw$ in graph H mirroring arrow v in graph G :

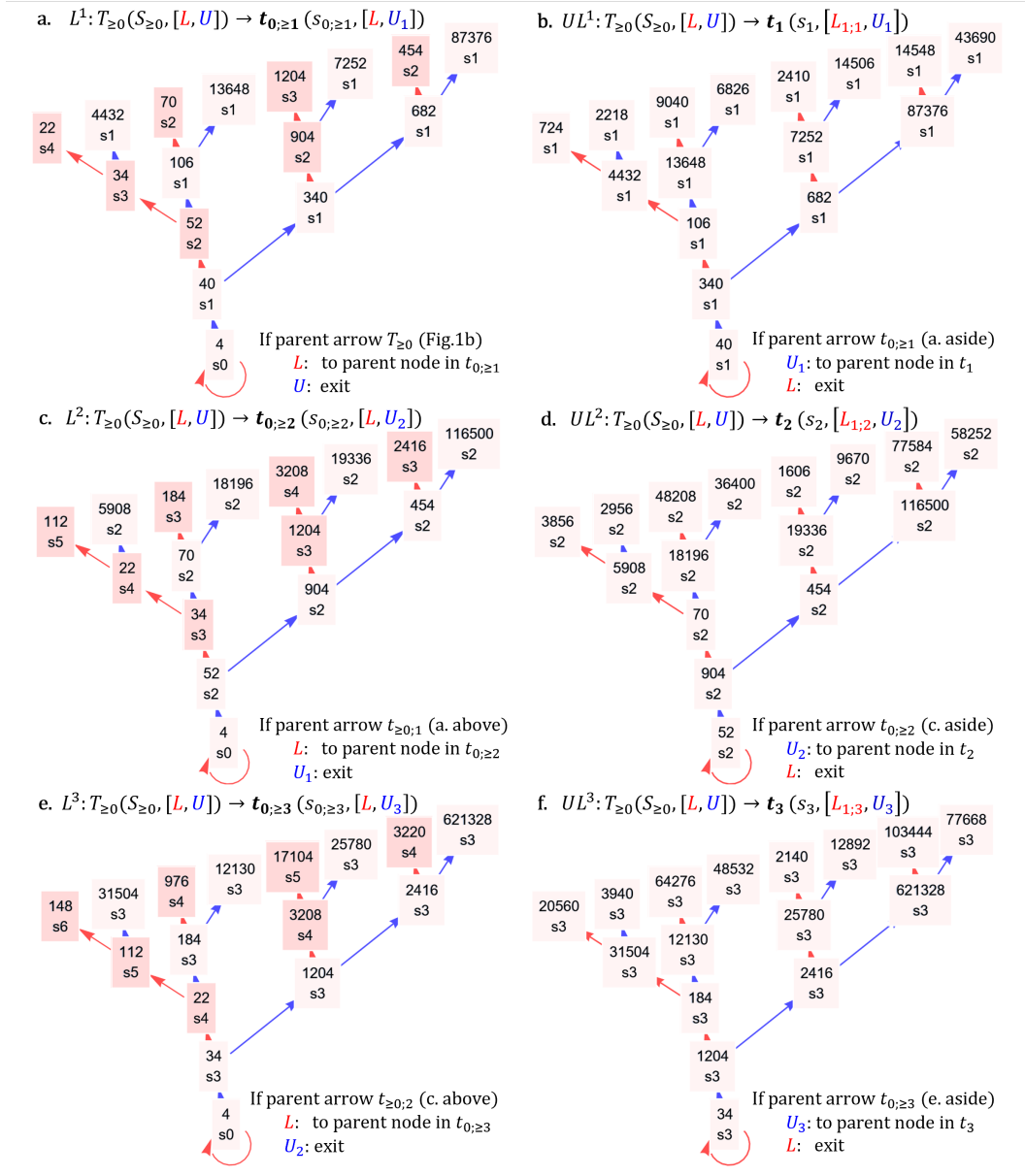
$$G \longrightarrow H$$

$$w : G \rightarrow H; v \rightarrow v_1 = w^{-1}vw \quad \text{or:} \quad \begin{array}{ccc} n & \xrightarrow{w} & w(n) \\ \uparrow v & & \uparrow v_1 = w^{-1}vw \\ m & \xrightarrow{w} & w(m) \end{array} \quad (3.17)$$

The subscript 1 in v_1 denotes that it is the first order conjugate of arrow v . A number of i iterations of walk w applied to v yields an i 'th order conjugate arrow $v_i = w^{-i}vw^i$. A walk mirroring itself is still the same walk, since: $w : w \rightarrow w^{-1}ww = w^0w = w$.

The arrow v in equation 3.17 represents the two different arrows L and U in the base graph $T_{\geq 0}$. They enable steps $v_1 = w^{-1}vw$ over generated inner arrows in generated leftward and upward *subtrees* (Figs.7ace,8ace) and *cotrees* (Figs.7bdf,8bdf) respectively (Def.3.7). The walks w of V-graph foot numbers connected by arrows v that are shortened to one inner $v_1 = w^{-1}vw$ arrow in the generated subtrees, were already specified as $L^{i=1,2,3,\dots}$ (Eq. 3.15), and $U^{j=1,2,3,\dots}$ (Eq.3.16).

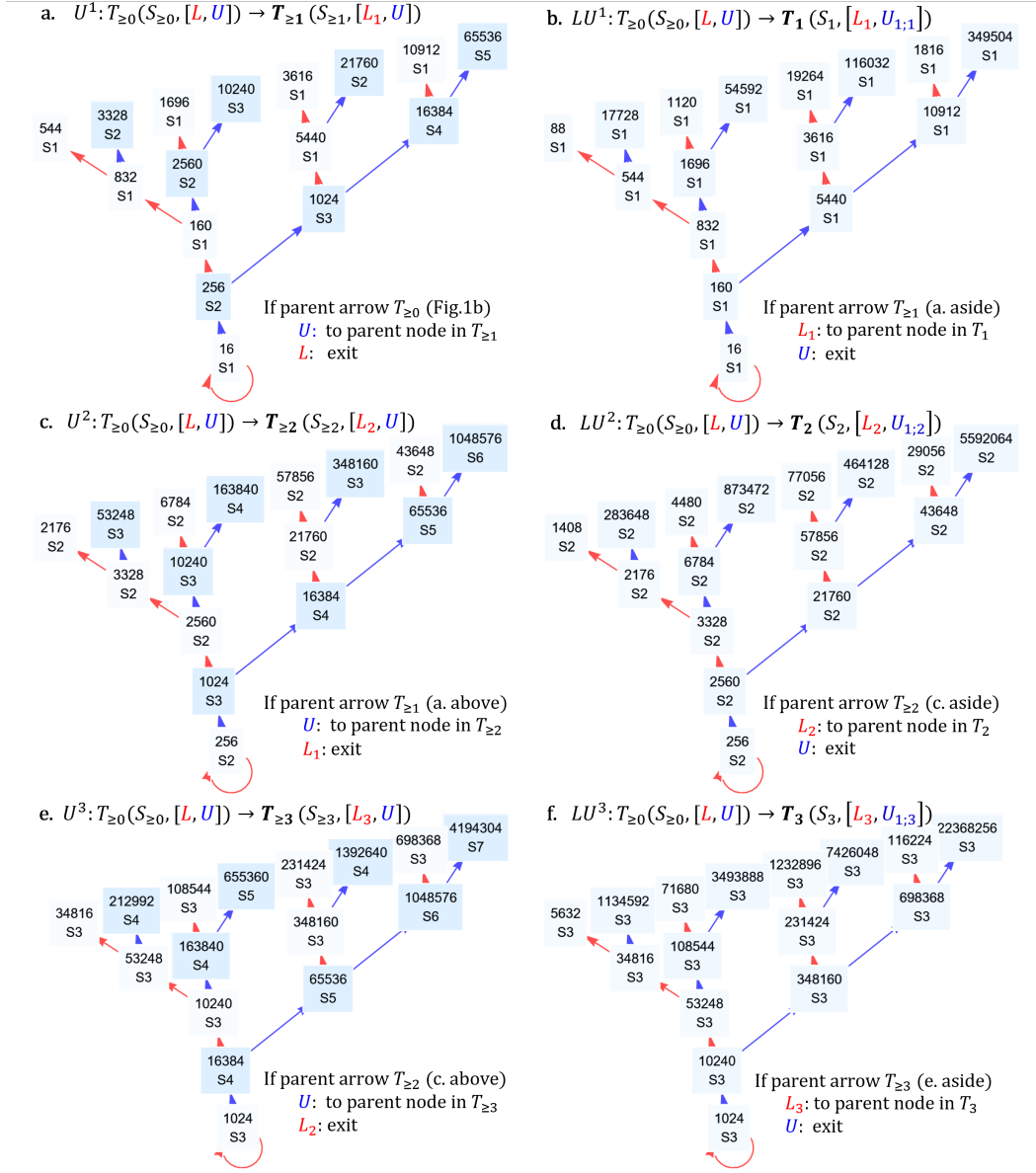
Figure 7: Leftward subtrees $t_{0;\geq i=1,2,3}$ and leftward cotrees $t_{i=1,2,3}$



Legend | Leftward moves $L^{i=1,2,3,\dots}$ of tree $T_{\geq 0}$ (Fig.1b) give leftward subtrees with nested generations (a) $s_{0;\geq 1}$ in $t_{0;\geq 1}$, (c) $s_{0;\geq 2}$ in $t_{0;\geq 2}$, (e) $s_{0;\geq 3}$ in $t_{0;\geq 3}$. Moves $UL^{i=1,2,3,\dots} = L^{i=1,2,3,\dots}U_i$ give leftward cotrees with disjoint generations (b) s_1 in t_1 , (d) s_2 in t_2 , (f) s_3 in t_3 . Leftward subtrees and cotrees obtain conjugate upward arrows $U_{i=1,2,3,\dots} = L^{-i}UL^i$; cotrees obtain conjugate leftward arrows $L_{i=1,2,3,\dots} = L^{-i}(U^{-1}LU)L^i$ via foot number detours, e.g.:

$$\begin{array}{ccccccc}
 256 \xrightarrow{L} 340 \xrightarrow{L} 904 \xrightarrow{L} 1204 \xrightarrow{L} \dots & ; & 40 \xrightarrow{U} 160 \xrightarrow{L} 106_{s1} \xrightarrow{L} 70_{s2} \xrightarrow{L} 184_{s3} \xrightarrow{L} \dots \\
 \uparrow^L & \uparrow^{U_1} & \uparrow^{U_2} & \uparrow^{U_3} & ; & \uparrow^L & \uparrow^{L_1} & \uparrow^{L_{1;1}} & \uparrow^{L_{1;2}} & \uparrow^{L_{1;3}} \\
 16 \xrightarrow{L} 40 \xrightarrow{L} 52 \xrightarrow{L} 34 \xrightarrow{L} \dots & & 16 \xrightarrow{U} 256 \xrightarrow{L} 340_{s1} \xrightarrow{U} 904_{s2} \xrightarrow{L} 1204_{s3} \xrightarrow{L} \dots \\
 T_{\geq 0} & t_{0;\geq 1} & t_{0;\geq 2} & t_{0;\geq 3} & & T_{\geq 0} & T_{\geq 1} & t_1 & t_2 & t_3
 \end{array}$$

Figure 8: Upward subtrees $T_{\geq i=1,2,3}$ and upward cotrees $T_{i=1,2,3}$



Legend | Upward moves $U^{j=1,2,3,\dots}$ of tree $T_{\geq 0}$ (Fig.1b) give upward subtrees with nested generations (a) $S_{\geq 1}$ in $T_{\geq 1}$, (c) $S_{\geq 2}$ in $T_{\geq 2}$, (e) $S_{\geq 3}$ in $T_{\geq 3}$. Moves $LU^{j=1,2,3,\dots} = U^{j=1,2,3,\dots}L_j$ give upward cotrees with disjoint generations (b) S_1 in T_1 , (d) S_2 in T_2 , (f) S_3 in T_3 . Upward subtrees and cotrees obtain conjugate leftward arrows $L_{j=1,2,3,\dots} = U^{-j}LU^j$; cotrees obtain conjugate upward arrows $U_{j=1,2,3,\dots} = U^{-j}(L^{-1}UL)U^j$ via foot number detours, e.g.:

$$\begin{array}{ccccccc}
 40 \xrightarrow{U} 160 \xrightarrow{U} 2560 \xrightarrow{U} 10240 \xrightarrow{U} \dots & ; & 256 \xrightarrow{L} 340 \xrightarrow{U} 5440_{S_1} \xrightarrow{U} 21760_{S_2} \xrightarrow{U} 348160_{S_3} \xrightarrow{U} \dots \\
 \uparrow^L & \uparrow^{L_1} & \uparrow^{L_2} & \uparrow^{L_3} & \uparrow^U & \uparrow^{U_1} & \uparrow^{U_{1;1}} & \uparrow^{U_{1;2}} & \uparrow^{U_{1;3}} \\
 T_{\geq 0} & T_{\geq 1} & T_{\geq 2} & T_{\geq 3} & T_{\geq 0} & t_{0;\geq 1} & T_1 & T_2 & T_3
 \end{array}$$

Definition 3.7. *Inner arrows of leftward and upward subtrees* (Figs.7ace and 8ace)

$$L^{i=1,2,3,\dots} : T_{\geq 0}(S_{\geq 0}, [L, U]) \rightarrow t_{0;\geq i}(s_{0;\geq i}, [U_i, L]) \quad \text{in which } U_i = L^{-i}UL \quad (3.18)$$

$$U^{j=1,2,3,\dots} : T_{\geq 0}(S_{\geq 0}, [L, U]) \rightarrow T_{\geq j}(S_{\geq j}, [U, L_j]) \quad \text{in which } L_j = U^{-j}LU^j \quad (3.19)$$

The inner arrows of leftward and upward *cotrees* (Figs.7bdf,8bdf) result from the walks w of foot numbers of V-graphs to the two infinite series of their arm numbers. These walks are specified as $UL^{i=1,2,3,\dots}$ (Eq.3.13) and $LU^{j=1,2,3,\dots}$ (Eq.3.14) respectively. These walks constitute the rows in the 4-regular middle pages graph G_{MP} (Fig.9).

Definition 3.8. *Inner arrows of leftward and upward cotrees* (Figs.7bdf and 8bdf)

$$UL^{i=1,2,3,\dots} : T_{\geq 0}(S_{\geq 0}, [L, U]) \rightarrow t_{0;\geq i}(s_i, [U_i, L_{1;i}]) \quad (3.20)$$

$$\text{in which } L_{1;i} = L^{-i}(U^{-1}LU)L^i = L^{-i}L_1L^i \quad (3.21)$$

$$LU^{j=1,2,3,\dots} : T_{\geq 0}(S_{\geq 0}, [L, U]) \rightarrow T_{\geq j}(S_j, [U_{1;j}, L_j]) \quad (3.22)$$

$$\text{in which } U_{1;j} = U^{-j}(L^{-1}UL)U^j = U^{-j}U_1U^j \quad (3.23)$$

If the arrows in tree $T_{\geq 0}$ (Fig..1b) are considered as marriages, then each nephew-niece relation imposes an arrow in cotree t_1 or T_1 , each grand-nephew-grand-niece relation imposes an arrow in cotree t_2 or T_2 , each great-grand-nephew-great-grand-niece relation imposes an arrow in cotree t_3 or T_3 , and so on.

3.5 From cotrees to cotree skyscraper columns in the Middle Pages graph G_{MP}

Breadth-first orderings of the root paths of cotrees gives the columns on the middle pages parallel to the gutter column of the middle pages comprising the breadth-first ordered root paths of the Cayley graph $T_{\geq 0}$, to which the cotrees are isomorphic.

In a 1920 article [49], Emmy Noether (1882-1935) introduced that the study of congruence classes (Fig.10), Greatest Common Divisors and Least Common Multiple is helpful to understand non-commutative, regular, tree-like isomorphic structures (Fig.1b) in which stepping leftwards and climbing upwards next gives a different node than climbing upwards first and stepping leftwards next. Corollary 3.9 states that the non-commutativity of the 3-regular Cayley graph is not a feature anymore of its transformation to the 4-regular middle pages graph (Fig.9).

Corollary 3.9. *The 4-regular middle pages graph G_{MP} (Fig.9) is commutative.* Commutative means that the order of 4 step directions (the sequence of leftwards, rightwards, upwards and downwards steps) in paths towards a node does not matter [50, 51]. This order does not matter because each node in the 4-regular graph G_{MP} can be reached from these 4 directions from 4 different neighbour sites. \square

The *Skolem-Noether theorem* maintains that if and only if the transformation function (Eq.3.17) maps the inner arrows of a graph G one-by-one to those of its subgraphs, this graph G is *automorphic*, meaning that it is isomorphic to its subgraphs. The automorphism graph (Fig.11) is based on this insight.

Graph transformations are prominent in the recent literature. For example, with as goal a serial-to-parallel transformation of 'serial' arrows as in line graphs, to 'parallel' arrows as in star graphs, Ehrig [6] introduced *pushout* transformations. Generalizations thereof [9, 10] promise easy applicability. They just require the user to prevent or undo undesired transformations. For example, Jacob's ladder (Fig.5a), besides being transformed to its dual cotree skyscraper graph (Fig.5b), could have been transformed to parallel reachable binary numbers on its left stander, or to parallel reachable Collatz numbers on its right stander.

4 The 4-regular middle pages graph G_{MP}

The 4-regular middle pages graph (Fig.9) combines, in its columns, the breadth-first ordered skyscraper graphs of the 3-regular Cayley color graph (gutter, Fig.1b) and of its cotrees (left page, Figs.7, right page 8) with, in its rows, the walks of V-graph foot numbers to their V-arms numbers (Fig.6) in leftward generations s_1, s_2, s_3, \dots (left page) and in upward generations S_1, S_2, S_3, \dots (right page).

The 4-regular middle pages graph allows for *Eulerian round tours* of all number pairs of binary numbers representing root paths (Col. 2.4) and branching numbers reached by these root paths (next section, 5.12). Next to all branching numbers in the gutter of the graph and, once again, on the left page (leftward subtree columns) or the right pages (upward cotree columns), the 4-regular middle pages graph has as nodes *enumerators* with which the numbers on skyscraper graphs are connected in parallel, and via which they are connected to the trivial root. Whether such a parallel computer can be built or emulated does not matter here.

A maximum of k rewrites to check whether each of 2^{k-1} numbers converges to the trivial root

In the heuristic *term rewriting* approach [14, 15] numbers in Collatz root paths are written as binary numbers, of which the zeros and ones are pictured in the reverse order as black squares and white squares respectively. The root path to 31 in the Syracuse tree becomes a staircase of 39 steps with as first step the step from 1 : \square to 5 : $\square\square\square$ and as 39th step the step from 47 : $\square\square\square\square\square$ to 31 : $\square\square\square\square$. Jan-Willem Klop calculates the statistical expectation of the diminishment of the number of white squares at the front of the reversed digital number on the step below the current reversed digital number [15]. Based on this, probabilistic reasoning suggests that 1 in the trivial root "will always be reached, in all probability!".

Assuming already the proof of the Collatz conjecture (Col.2.4, 5.12) based on the middle pages graph (Fig.9), we dispose also of a proof for 2^k breadth-first ordered root paths for arbitrarily high exponents k , of which $2^k - 1$ with a root path length of k . This proof turns the fast heuristic approach for selected numbers into an even faster convergence check of k steps at most to the trivial root number pair $sm0c = 4$.

Let us *check* whether 31, with as $3n + 1$ image $3 \cdot 31 + 1 = 94$, converges to the trivial root indeed based on leftward and upward steps, rather than Syracuse function steps. 94 was already signalled as the lowest of 9 numbers 94, 124, 142, 166, 214, 220, 250, 274, 286 lower than 288 not included in the Figure of the fractal binary tree based on root paths of $k = 18$ L and U arrows (Fig.4). The number 94 paired with its binary coded root path $^{1010^7 10^4 10^{26}}_{94}$ shares its root path length of 42 L or U steps with $2^{42-1} - 1 = 2\,199\,023\,255\,552 - 1 \approx 2.2$ trillion other numbers.

Step	1	2	3	4	5	6	7	8
V-arm number	16	10	101	1010^7	$1010^7 1$	$1010^7 10^4$	$1010^7 10^4 1$	$1010^7 10^4 10^{26}$
cotree	T_1	t_1	T_1	t_7	T_1	t_4	T_1	t_{26}
cotree root	16	10	16	10^7	16	10^4	16	10^{26}
		40		196		22		23293636

Table 1: 8 cotree switches to check the root path of $3 \cdot 31 + 1 = 94$ amidst 2^{42-1} root paths of 42 steps

The check uses 94's binary coded root path. Table 1 shows that the root path of 94 comprises 8 V-arm numbers in different cotree skyscraper columns of the breadth-first ordered cotrees T_1 (4x, Fig.8b), t_1 (Fig.7b), t_4 , t_7 and t_{26} , of which the cotree roots on the greedy branch and upward trunk are listed as well. All numbers in a cotree skyscraper column can be reached in parallel in the middle pages graph (Fig.9) from the enumerator functions below the columns. The binary numbers a representing the breadth-first ordered root paths a_x in the *V-arm number pair* row show that checking the existence of the root path of the number pair $^{1010^7 10^4 10^{26}}_{94}$ to the trivial root $^0_{4,30}$ requires only 8 switches between cotrees, corresponding to 8 subtractions $42 - (26 + 1 + 4 + 1 + 7 + 1 + 1 + 1) = 0$ from 42 yielding 0.

Figure 9: Middle pages graph G_{MP}

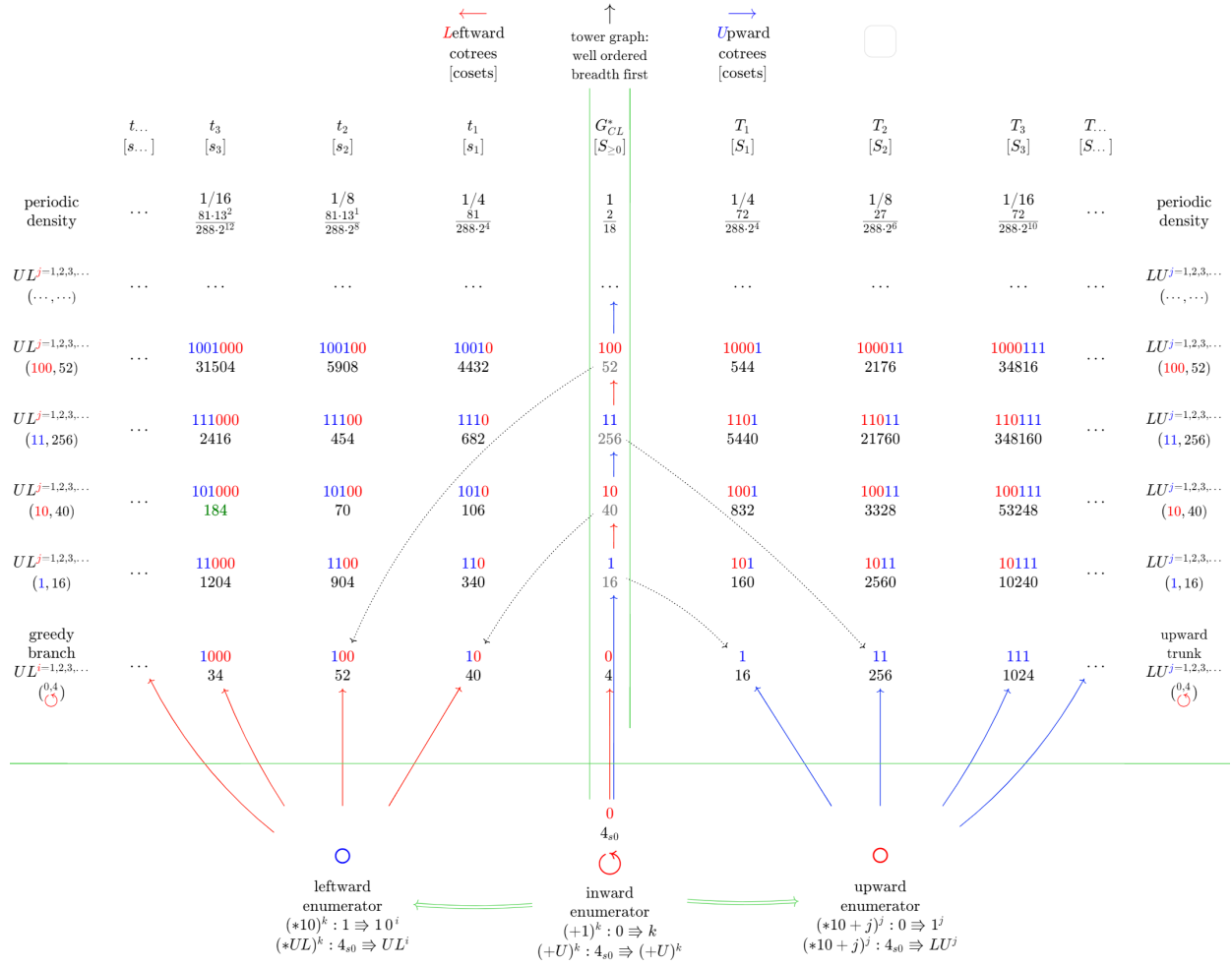


Fig. 9 | Legend. The gutter, or fold, between the two middle pages, contains the infinite skyscraper graph (Fig.5b) with $\frac{a}{x}$ numbers pairs of binary numbers a of breadth-first ordered root paths and the branching numbers x to which they lead. Each branching number is a foot number of a V-graph (Figs.1,6bd) that spreads its V-arms horizontally. Each V-arm number pair is reached horizontally from its V-foot number pair in the gutter. Each V-arm number pair is also part of its skyscraper graph column representing the breadth-first ordered root paths in its own cotree. The left page columns s_1, s_2, s_3, \dots are breadth-first ordered cosets per leftward successor generation at the nodes of leftward cotrees t_1, t_2, t_3, \dots (Fig.7). The right page columns S_1, S_2, S_3, \dots are breadth-first ordered cosets per upward successor generation on the nodes of upward cotrees T_1, T_2, T_3, \dots (Fig.8).

A top row shows the *periodic density* for the columns with skyscraper tapes of leftward cotrees and rightward cotrees. The cumulative density of binary numbers representing breadth-first ordered root paths in both leftward and upward cotrees is $1/4 + 1/8 + 1/16 + \dots = 1/2$ (Col.2.4). The density of branching numbers paired to them amounts $27/288$ (Eq.5.11) respectively $5/288$ (Eqs.5.9,5.10), which adds up to the density of all branching numbers $32/188 = 2/18$ (Fig.5.12) . |

5 The Collatz congruence classes graph $G_{CC} = ([0, \dots, 17]_{18}, [f, g])$

Elementary *modular arithmetic* from the field of number theory [30, 31] is required to define for an $an + b$ function branching numbers and non-branching numbers, the L , U and F functions that connect them, as well as the numbers on the nodes of subtrees and cotrees. Modular arithmetic is arithmetic with *congruence classes*, shortly *classes*, of numbers having the same remainder after division by a divisor, modulus, or *periodicity*. A class $[a]_b$ contains the natural numbers with a remainder of a after division by b .

The odd numbers not divisible by 3 constitute the classes $[1, 5]_6$. The Collatz subfunction $f^{-1} : n \rightarrow 3n + 1$ applied to the classes $[1, 5]_6$ therefore yields the set of branching numbers $S_{\geq 0}$ with two branching children.

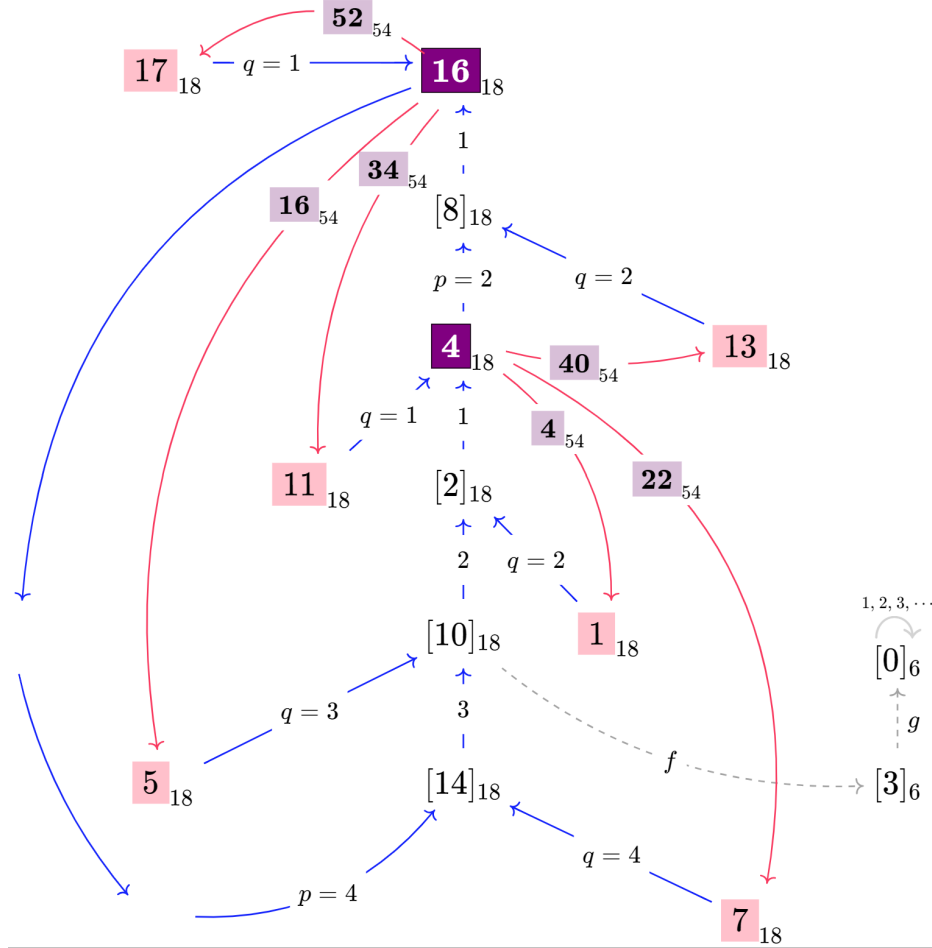
$$f^{-1} : [1, 5]_6 \rightarrow [3 \cdot 1 + 1, 3 \cdot 5 + 1]_{3 \cdot 6} = [4, 16]_{18}, \quad \text{yielding: } S_{\geq 0} = [4, 16]_{18} \quad (5.1)$$

The branching classes consist of the arithmetic progressions $4, 22, 40, \dots$ and $16, 34, 52, \dots$ with a periodicity of 18, or alternatively, of each number n with a congruence relation of either $4 \equiv n \pmod{18}$ or $16 \equiv n \pmod{18}$ to the numbers 4 respectively 16. Their *periodic density* amounts to $2/18$, meaning that 2 out of 18 successive numbers is a branching number, regardless whether just one or an arbitrarily large number of periods of length 18 is considered. The directed Collatz congruence classes graph (Fig.5) has as nodes the congruence classes $[0, \dots, 17]_{18}$ modulo 18.

$$G_{cc} = ([0, \dots, 17]_{18}, [f, g]), \quad \text{with } f : n \rightarrow (n-1)/3; \quad g : n \rightarrow 2n \quad (5.2)$$

Fig.10 shows the sequence of $g : n \rightarrow 2n$ arrows (Fig.5, blue or grey) and $f : n \rightarrow (n-1)/3$ arrows (Fig.5, red or grey) in each of the different paths from the argument (sub)classes of a function towards one of the purple-coloured branching classes $[4]_{18}$ and $[16]_{18}$. Allowing the classes $[4, 16]_{18}$ to branch by $f : n \rightarrow (n-1)/3$ to the odd classes $[1, 7, 13], [5, 11, 17]_{18}$ requires the branching subclasses $S_{\geq 0} = [[4, 22, 40], [16, 34, 52]]_{54}$ with a three times higher periodicity of $3 \cdot 18 = 54$ (Def.5.2). The red f -arrows are labelled with these subclasses. Each path from one branching class to another is labelled with a number q or a number of p of successive $g : n \rightarrow 2n$ arrows, depending on whether the first arrow is a $f : n \rightarrow (n-1)/3$ arrow (Fig.3, red) or not.

Figure 10: The Collatz congruence classes graph $G_{cc} = ([0, \dots, 17]_{18}, [f, g])$



Legend | The arrows represent the functions $f : n \rightarrow (n-1)/3$ (red or grey) and $g : n \rightarrow 2n$ (blue or grey). For example, $g : [14]_{18} \rightarrow [10]_{18}$, since $2 \cdot 14$ divided by 18 has remainder 10. Walks to one of the purple coloured branching classes $[4]_{18}$ and $[16]_{18}$ can be made from 16 non-branching classes modulo 18, subdivided into 6 red-coloured odd classes, 6 classes divisible by 3 combined in the classes $[3]_6 = [3, 9, 15]_{18}$ and $[0]_6 = [0, 6, 12]_{18}$, and in 4 non-coloured non-branching even classes. Numbers in arrow headings represent the number of g steps to the next branching class, thus $[14]_{18} \xrightarrow{3} \dots \rightarrow [4]_{18}$ represents $g^3 : [14]_{18} \rightarrow [4]_{18}$ (Def.3). Starting from the two branching classes $[4, 16]_{18}$, the arrow headings $\vec{p} = [2, 4]$ specify the upward function $U = g^p$ (Def.1). Starting from the branching subclasses $[4, 16, 22, 34, 40, 52]_{54}$ shown on the red-coloured f arrows to the odd classes $[1, 5, 7, 11, 13, 17]_{18}$, the arrow headings $\vec{q} = [2, 3, 4, 1, 2, 1]$ specify the leftward function $L = fg^q$ (Def.2). Walks starting from a class divisible by 3 start with reverse arrows, for example $f^{-1}g^2 : [3]_6 \rightarrow [4]_{18}$ (Def.3). |

5.1 Defining the Leftward, Upward and Forward functions

The arrows without a p or q label define the function F by which different congruence classes of non-branching numbers walk to the branching classes (Def.5.5). A close inspection of the p and q label in Fig.10 yields the definitions of the upward function (Def.5.1) and the leftward function (Def.5.2).

The upward function U

The upward function U (Def.5.1) is specified differently for the two branching classes $[4]_{18}$ and $[16]_{18}$ in set $S_{\geq 0}$ (Def.5.1). In Fig.10, the p -number on the first $g : n \rightarrow 2n$ arrow in a path of p successive blue-coloured g arrows from one of these two branching classes to the other shows the power p to which 2 is raised in $U = g^p : n \rightarrow n \cdot 2^p$

Definition 5.1. Upward function $U : S_{\geq 0} \rightarrow S_{\geq 1}; n \rightarrow (ng^p = n \cdot 2^p)$

$S_{\geq 0}$	p	:	$U(n)$;	$S_{\geq 1}$	=	$[c5]_{288} = [c5(1,4)]_{288}$;	\vec{h}_U
$[4]_{18}$	2	:	$ng^2 = 4n$;	$[16]_{72}$	=	$[16, 88, 160, 232]_{288}$;	4
$[16]_{18}$	4	:	$ng^4 = 16n$;	$[256]_{288}$	=	$[256]_{288}$;	1

The different powers $p = 2$ and $p = 4$ for the classes $[4]_{18}$ and $[16]_{18}$ yield upward output classes $[16]_{72}$ and $[256]_{288}$ with different intrinsic periodicities $72 = 2^3 3^2$ and $288 = 2^5 3^2$ of the numbers in them. These intrinsic periodicities have as their Least Common Multiple periodicity $\text{LCMp} = 2^5 3^2 = 288$. The upward alignment vector $\vec{h}_{U1} = [4, 1]$ expresses that $4 + 1 = 5$ upward numbers occur in each successive LCM period of 288 natural numbers, The set of upward numbers $S_{\geq 1}$ therefore consists of five classes with $\text{LCMp} = 288$:

$$S_{\geq 1} = [[256], [16, 88, 160, 232]_{288}, \text{ denoted as: } [c5]_{288} \text{ or as: } [c5(1,4)]_{288} \quad (5.3)$$

The notation $c5(1,4)$ means that 1 out of the 5 upward classes belongs to branching class $[4]_{18}$, while 4 of them belong to branching class $[16]_{18}$. Only $[256]_{288}$ belongs to $[4]_{18}$.

The periodicity expansion by one upward iteration, denoted as θ_{U1} , is obtained by dividing the periodicity of upward numbers, which is 288, by the periodicity of branching number arguments, which is 18. The periodicity expansion by two upward iterations, denoted as θ_{U2} , can already be seen from Figure 10. The two branching classes are interconnected by an upward cycle of six blue-coloured $g : n \rightarrow 2n$ arrows.

$$\theta_{U1} = 288/18 = 16; \quad \theta_{U2} = 6, \text{ implying that: } U^2 : n \rightarrow 2^{3 \cdot 2} n, \text{ or: } U^2(n) = 64n \quad (5.4)$$

Since $U^2(n) = 64n$ always holds, we will distinguish the output classes and periodicities of successive *odd upward iterations* $U^{1,3,5,\dots}$ from those of successive *even upward iterations* $U^{2,4,6,\dots}$.

The leftward function L

The leftward function L (eq.5.2) requires a three times higher argument periodicity than the periodicity 18 of the branching classes $[4, 18]_{18}$ to obtain six branching subclasses $[4, 16, 22, 34, 40, 52]_{54}$. Applied to them, the red-coloured $f : n \rightarrow (n-1)/3$ arrows in Fig.10 yield six odd classes $[1, 5, 7, 11, 13, 17]_{18}$ with again a periodicity of 18. The q -number on the first $g : n \rightarrow 2n$ arrow in a path from one branching class to another consisting of the red-coloured f -arrow followed by q successive blue-coloured g arrows shows the power q to which 2 is raised in the leftward function $L = fg^q : n \rightarrow n \cdot (n-1)/3 \cdot 2^q$.

Definition 5.2. Leftward function $L : S_{\geq 0} \rightarrow s_{0;\geq 1}; n \rightarrow (nfg^q = (n-1)/3 \cdot 2^q)$

$S_{\geq 0}$	q	:	$L(n)$:	$s_{0;\geq 1}$	=	$[c27]_{288} = [c27(15, 12)]_{288}$:	\vec{h}_L
$[4]_{54}$	2	:	$nfg^2 = 4(n-1)/3$:	$[4]_{72}$	=	$[4, 76, 148, 220]_{288}$:	4
$[16]_{54}$	3	:	$nfg^3 = 8(n-1)/3$:	$[40]_{144}$	=	$[40, 184]_{288}$:	2
$[22]_{54}$	4	:	$nfg^4 = 16(n-1)/3$:	$[112]_{288}$	=	$[112]_{288}$:	1
$[34]_{54}$	1	:	$nfg^1 = 2(n-1)/3$:	$[22]_{36}$	=	$[22, 58, 94, 130, 166, 202, 238, 274]_{288}$:	8
$[40]_{54}$	2	:	$nfg^2 = 4(n-1)/3$:	$[52]_{72}$	=	$[52, 124, 196, 268]_{288}$:	4
$[52]_{54}$	1	:	$nfg^1 = 2(n-1)/3$:	$[34]_{36}$	=	$[34, 70, 106, 142, 178, 214, 250, 286]_{288}$:	8

The different powers q for the six subclasses modulo 54 yield leftward output classes with different intrinsic periodicities $36 = 2^2 3^2$, $72 = 2^3 3^2$, $144 = 2^4 3^2$ and $288 = 2^5 3^2$ of the numbers in them. These intrinsic periodicities have as their Least Common Multiple periodicity $\text{LCMp} = 2^5 3^2 = 288$. The leftward alignment vector $\vec{h}_R = [4, 2, 1, 8, 4, 8]$ indicates that in total 27 leftward numbers occur in each successive LCM period of 288 natural numbers, The set of leftward numbers $s_{0;\geq 1}$ therefore consists of 27 classes with $\text{LCMp} = 288$:

$$s_{0;\geq 1} = \left[\begin{array}{c} [4, 22, 40, 58, 76, 94, 112, 130, 148, 166, 184, 202, 220, 238, 274], \\ [34, 52, 70, 106, 124, 142, 178, 196, 214, 250, 268, 286] \end{array} \right]_{288} \quad (5.5)$$

denoted as: $[c27]_{288}$, or as: $[c27(15, 12)]_{288}$

The notation $c27(15, 12)$ means that 15 out of the 27 leftward classes belong to branching class $[4]_{18}$, while 12 of them belong to branching class $[16]_{18}$. The leftward expansion factor, denoted as $\theta_L = 163$ is obtained by dividing the leftward periodicity 288 by the branching periodicity 16, but at each leftward iteration the argument periodicity is increased by a factor 3, which yields as leftward output periodicity expansion given a three times higher argument periodicity.

$$3\theta_L = 16 \quad (5.6)$$

Corollary 5.3. Upward and leftward classes are disjoint. The upward classes $S_{\geq 1} = [c5]_{288}$ and leftward classes $s_{0;\geq 1} = [c27]_{288}$ do not share a single congruence class modulo 288, and therefore not a single number, as can be seen by comparing their listings (Eq.5.3,5.5).

Remark 5.4. Why 0 is included in the subscript of the subsets generated by leftward iterations. The root set s_0 is conjectured to include only the trivial root $c = 4_{s_0}$. Numbers from set s_0 are defined as leftward numbers with only leftward numbers as their ancestors; they have no different-colour ancestor. Therefore leftward iterations $L^{i=1,2,3,\dots} : s_0 \rightarrow s_0$ do not push out numbers from set s_0 . Since set s_0 is not pushed out by leftward iterations, a 0 is included in the subscript of the output set, for example: $L^4 : S_{\geq 0} \rightarrow S_{0;\geq 4}$.

The forward function F

Fig.10 also shows the sequences of f -, g -, f^{-1} -, and g^{-1} -arrows that specify the composite function F for a walk of numbers from the 16 non-branching classes to a number from the two branching classes (Def.5.5).

Arrows g^{-1} and f^{-1} that bring numbers closer to the trivial root show up in the paths of number classes divisible by 3. For odd number classes the walk to a branching number is specified in Fig.10 by the q -arrows. For the uncoloured even non-branching classes $[2, 8]_{16}$, $[10]_{14}$ and $[14]_{18}$ the number of blue-coloured g -arrows towards the next branching class is shown in Fig.10 by the power of 2 on the first arrow, e.g. $[10]_{18} \xrightarrow{2} \dots [4]_{18}$ means $g^2 : [10]_{18} \rightarrow [4]_{18}$.

Definition 5.5. Forward function $F : [0, 1, 2, 3, 5 \dots 15, 17]_{18} \rightarrow S_{\geq 0}; n \rightarrow F(n)$

Non-branching class	r	:		$F(n)$	$S_{\geq 0}$
$[3]_6 = [3, 9, 15]_{18}$	2	:	$nf^{-1}g^2$	$= 12n + 4$	$[4]_{18}$
$[0]_6 = [0, 16, 12]_{18}$	2	:	$ng^{-i}f^{-1}g^2$	$= 12n / 2^{i=1,2,3,\dots} + 4$	$[4]_{18}$
$[2, 8, 11, 17]_{18}$	1	:	ng^1	$= 2n$	$[4, 16]_{18}$
$[1, 10, 13]_{18}$	2	:	ng^2	$= 4n$	$[4, 16]_{18}$
$[5, 14]_{18}$	3	:	ng^3	$= 8n$	$[4]_{18}$
$[7]_{18}$	4	:	ng^4	$= 16n$	$[4]_{18}$

Lemma 5.6. Every number in each of the 16 non-branching classes $[0, \dots, 3, 5, \dots, 15, 17]_{18}$ can complete the walk to a number in the branching classes $S_{\geq 0} = [4, 16]_{18}$ on the nodes of the Cayley colour graph $T_{\geq 0} = (S_{\geq 0}, [L, U])$. **Proof:** For all numbers from each of the 16 non-branching classes $[0, \dots, 3, 5, \dots, 15, 17]_{18}$ the forward function (Def.5.5) shows that function F yields a walk to a branching number from the branching classes $S_{\geq 0} = [4, 16]_{18}$. \square

Specification of tree $T_{\geq 0}$

The Cayley colour graph $T_{\geq 0} = (S_{\geq 0}, [L, U])$ (Fig.1b) can now be further defined with the delineations of upward and leftward number classes (Table 1) in the definitions of U and L .

$$T_{\geq 0} = (S_{\geq 0}, [L, U]) = ([s_{0;\geq 1}, S_{\geq 1}], [L, U]) = ([c27, c5]_{288}, [L, U]) \quad (5.7)$$

The functions L and U divide the classes $S_{\geq 0}$ in leftward classes $s_{\geq 0} = [c27]_{288}$ and upward classes $S_{\geq 1} = [c5]_{288}$. The notation of sets of classes allows for the assessment of their *periodic density* (Def.1.3) by simply dividing the number of classes in their name by their periodicity. Periodic densities of disjoint sets of classes can be added, for example those of the disjoint non-branching and branching classes, and those of disjoint leftward and upward classes.

Corollary 5.7. Periodic densities of:

$$\begin{aligned} \text{binary numbers left stander skyscraper grph (2.4) :} & \quad d(\mathbb{N}) = 1 \\ \text{non-branching numbers, branching numbers :} & \quad d([0, 1, 2, 3, 5, \dots, 15, 17]_{18}) = 16/18, \\ & \quad d(S_{\geq 0}) = d([4, 16]_{18}) = 2/18 = 32/288 \\ \text{leftward numbers, upward numbers :} & \quad d(s_{0;\geq 1}) = d([c27]_{288}) = 27/288, \\ & \quad d(S_{\geq 1}) = d([c5]_{288}) = 5/288 \end{aligned}$$

The next step is to specify the congruence classes generated by the subtree generating functions L^i and U^j and the cotree generating functions UL^i and LU^j .

5.2 Periodicities of leftward and upward subtrees and cotrees

The periodicities of the numbers on the nodes of subtrees and cotrees follow from the composite functions L^i , U^j , UL^i and LU^j that also generate their node sets their inner arrows (Def.3.7-3.8).

Successive subtrees and cotrees obtain number classes on their nodes with successively higher Least Common Multiple periodicities (LCMp's). Corresponding subtrees and cotrees share their LCMp-expansions. The node sets of Leftward trees, even upward trees and odd upward trees show different LCMp-expansions.

The LCMp's of *upward* subtrees and cotrees follow from the periodicity expansions $\theta_{U1} = 2^4$ for a single (first) upward iteration U^1 and $\theta_{U2} = 2^{3 \cdot 2}$ for two upward iterations U^2 . Two upward iterations

always yield expansion by $2^{3 \cdot 2} = 64$ since $U^2(n) = 2^{3 \cdot 2}n$ (Def.5.1). As a result, the periodicities of the *even upward* subtrees and cotrees can be considered separately from the periodicities of the *odd upward* subtrees and cotrees. Both the density decay of successive even subtrees and cotrees, and the density decay of successive odd subtrees and cotrees, amounts to $r_{U2} = 1/2^{3 \cdot 2} = 1/64$.

The LCMp's of *leftward* subtrees and cotrees follow from the leftward output expansion $3\theta_R = 16 = 2^4$ per iteration. The leftward output expansion by $3\theta_R$ at each iteration requires an argument period expansion by 3 at each iteration. A three times higher argument periodicity at each leftward iteration guarantees leftward walks via three different odd classes modulo 18 to $3 \cdot 288 \cdot 2^{4i}$ (Fig.10) leftward numbers.

Corollary 5.8. LCM periodicities of leftward and upward subsets and cosets (Figs.7, 8)

$$\theta_{U2} = 2^{3 \cdot 2}, \text{ LCMp even upward subtrees: } U^{j=2,4,6,\dots} : [S_{\geq 0}]_{288} \rightarrow [S_{\geq j}]_{288 \cdot 2^{3j}} \quad (5.8)$$

$$\text{cotrees: } LU^{j=2,4,6,\dots} : [S_{\geq 0}]_{288} \rightarrow [S_j]_{288 \cdot 2^{3j}} \quad (5.9)$$

$$\theta_{U1} = 2^4, \theta_{U2} = 2^{3 \cdot 2}, \text{ LCMp odd upward subtrees: } U^{j=1,3,5,\dots} : [S_{\geq 0}]_{288} \rightarrow [S_{\geq j}]_{288 \cdot 2^{3j+1}} \quad (5.10)$$

$$\text{cotrees: } LU^{j=1,3,5,\dots} : [S_{\geq 0}]_{288} \rightarrow [S_j]_{288 \cdot 2^{3j+1}} \quad (5.11)$$

$$3\theta_R = 2^4, \text{ LCMp leftward subtrees: } L^{i=1,2,3,\dots} : [S_{\geq 0}]_{288} \rightarrow [s_{0 \geq i}]_{3 \cdot 288 \cdot 2^{4i}} \quad (5.12)$$

$$\text{cotrees: } UL^{i=1,2,3,\dots} : [S_{\geq 0}]_{288} \rightarrow [s_i]_{3 \cdot 288 \cdot 2^{4i}} \quad (5.13)$$

Table 2 lists the four sets $c351, c81, c72$, and $c8$ of the congruence classes of the nodes of first two subtrees $t_{\geq 1}$ and $T_{\geq 1}$. These four sets underlie the classes of all other subtrees and cotrees. *Cotree density* is calculated as the number of classes relative to the periodicity of a cotree. The automorphism graph (Fig.11) is annotated with the cotree densities $d(T_1) = 72/(288 \cdot 2^4)$, $d(T_2) = 27/(288 \cdot 2^6)$ and $d(t_1) = 81/(288 \cdot 2^4)$. The notation $[c72]_{288 \cdot 2^4}$ for the classes of T_1 elucidates that $d(T_1) = 72/(288 \cdot 2^4)$ indeed. The geometric sum formula $s = a/(1 - r)$ applies to the cumulative densities $1/672$ and $1/63$ of even and odd upward cotree numbers, and $27/288$ of leftward cotree numbers (5.12).

Table 2: Six base sets of congruence classes of subtrees and cotrees

$S_{\geq 0} = [4, 16]_{18}$, argument classes U , alignment vector to lcm-p=288 is $\vec{h}_U = [4, 1]$
 $S_{\geq 0} = [4, 16, 22, 34, 40, 52]_{54}$, argument subclasses L , alignment vector to lcm-p is $\vec{h}_R = [4, 2, 1, 8, 4, 8]$

$T_{\geq 0}[c27(15, 12), c5(1, 4)]_{288}$, leftward and upward classes $T_{\geq 0}[s_{\geq 0}, S_{\geq 1}]$ by argument classes $[4, 16]_{18}$
 $[c27(15, 12)]_{288} = [[4, 22, 40, 58, 76, 94, 112, 130, 148, 166, 184, 202, 220, 238, 274],$
 $[34, 52, 70, 106, 124, 142, 178, 196, 214, 250, 268, 286]]_{288}$
 $[c5(1, 4)]_{288} = [[256], [16, 88, 160, 232]]_{288}$

$T_{\geq 1}[c72, c8]_{288, 2^4}$ upward coset S_1 and subset $S_{\geq 2}$ in the first (odd) upward subtree $T_{\geq 1}[S_1, S_{\geq 2}]$
 $[c72]_{288, 2^4} = [16, 88, 160, 232, 304, 376, 448, 520, 544, 592, 664, 736,$
 $808, 832, 880, 952, 1096, 1120, 1168, 1240, 1312, 1384, 1456, 1528,$
 $1600, 1672, 1696, 1744, 1816, 1888, 1960, 1984, 2032, 2104, 2248, 2272,$
 $2320, 2392, 2464, 2536, 2608, 2680, 2752, 2824, 2848, 2896, 2968, 3040,$
 $3112, 3136, 3184, 3256, 3400, 3424, 3472, 3544, 3616, 3688, 3760, 3832,$
 $3904, 3976, 4000, 4048, 4120, 4192, 4264, 4288, 4336, 4408, 4552, 4576]_{288, 2^4}$
 $[c8]_{288, 2^4} = [256, 1024, 1408, 2176, 2560, 3328, 3712, 4480]_{288, 2^4}$

$t_{0, \geq 1}[3c351, 3c81]_{288, 3, 2^4}$ leftward subset $s_{0, \geq 2}$ and coset s_1 in the first leftward subtree $t_{0, \geq 1}[s_1, s_{0, \geq 2}]$
 $[c351]_{288, 2^4} = [4, 22, 34, 52, 70, 76, 94, 112, 124, 130, 142, 148, 166, 178,$
 $184, 196, 214, 220, 238, 268, 274, 286, 292, 310, 322, 328, 358,$
 $364, 382, 400, 412, 418, 430, 436, 454, 466, 472, 484, 502, 508, 526,$
 $556, 562, 574, 580, 598, 610, 628, 646, 652, 670, 688, 700, 706,$
 $718, 742, 754, 760, 772, 790, 796, 814, 844, 850, 862, 868, 886, 898,$
 $904, 916, 934, 940, 958, 976, 988, 994, 1006, 1012, 1030, 1042, 1048,$
 $1060, 1078, 1084, 1102, 1132, 1138, 1150, 1156, 1174, 1186, 1204, 1222, 1228, 1246,$
 $1264, 1276, 1282, 1294, 1300, 1318, 1330, 1336, 1348, 1366, 1372, 1390, 1420,$
 $1426, 1438, 1444, 1462, 1474, 1480, 1510, 1516, 1534, 1552, 1564, 1570, 1582, 1588,$
 $1606, 1618, 1624, 1636, 1654, 1660, 1678, 1708, 1714, 1726, 1732, 1750, 1762,$
 $1780, 1798, 1804, 1822, 1840, 1852, 1858, 1870, 1894, 1906, 1912, 1924, 1942, 1948,$
 $1966, 1996, 2002, 2014, 2020, 2038, 2050, 2056, 2068, 2086, 2092, 2110, 2128,$
 $2140, 2146, 2158, 2164, 2182, 2194, 2200, 2212, 2230, 2236, 2254, 2284, 2290, 2302,$
 $2308, 2326, 2338, 2356, 2374, 2380, 2398, 2416, 2428, 2434, 2446, 2452, 2470,$
 $2482, 2488, 2500, 2518, 2524, 2542, 2572, 2578, 2590, 2596, 2614, 2626, 2632, 2662,$
 $2668, 2686, 2704, 2716, 2722, 2734, 2740, 2758, 2770, 2776, 2788, 2806, 2812,$
 $2830, 2860, 2866, 2878, 2884, 2902, 2914, 2932, 2950, 2956, 2974, 2992, 3004, 3010,$
 $3022, 3046, 3058, 3064, 3076, 3094, 3100, 3118, 3148, 3154, 3166, 3172, 3190,$
 $3202, 3208, 3220, 3238, 3244, 3262, 3280, 3292, 3298, 3310, 3316, 3334, 3346, 3352,$
 $3364, 3382, 3388, 3406, 3436, 3442, 3454, 3460, 3478, 3490, 3508, 3526, 3532,$
 $3550, 3568, 3580, 3586, 3598, 3604, 3622, 3634, 3640, 3652, 3670, 3676, 3694, 3724,$
 $3730, 3742, 3748, 3766, 3778, 3784, 3814, 3820, 3838, 3856, 3868, 3874, 3886,$
 $3892, 3910, 3922, 3928, 3940, 3958, 3964, 3982, 4012, 4018, 4030, 4036, 4054, 4066,$
 $4084, 4102, 4108, 4126, 4144, 4156, 4162, 4174, 4198, 4210, 4216, 4228, 4246,$
 $4252, 4270, 4300, 4306, 4318, 4324, 4342, 4354, 4360, 4372, 4390, 4396, 4414, 4444,$
 $4450, 4462, 4468, 4486, 4498, 4504, 4516, 4534, 4540, 4558, 4588, 4594, 4606]_{288, 2^4}$
 $[c81]_{288, 2^4} = [40, 58, 106, 202, 250, 340, 346, 394, 490, 538, 616, 634, 682, 724,$
 $778, 826, 922, 970, 1066, 1114, 1192, 1210, 1258, 1354, 1402, 1492, 1498,$
 $1546, 1642, 1690, 1768, 1786, 1834, 1876, 1930, 1978, 2074, 2122, 2218, 2266, 2344,$
 $2362, 2410, 2506, 2554, 2644, 2650, 2698, 2794, 2842, 2920, 2938, 2986, 3028,$
 $3082, 3130, 3226, 3274, 3370, 3418, 3496, 3514, 3562, 3658, 3706, 3796, 3802, 3850,$
 $3946, 3994, 4072, 4090, 4138, 4180, 4234, 4282, 4378, 4426, 4432, 4522, 4570]_{288, 2^4}$

Congruence classes and densities of even upward subtrees and cotrees

The congruence classes of the numbers on the nodes of subtrees and cotrees follow from the composite functions L^i , U^j , UL^i and LU^j that also generate their node sets, their inner arrows and their periodicities (Eqs.3.15,3.16,3.11,3.12).

Since $U^2(n) = 2^{3 \cdot 2}n$ (Def.5.1), two upward iterations always yield an expansion by $2^{3 \cdot 2} = 64$. For example, the leftward class $[22]_{288}$ in $T_{\geq 0}$ is mapped in subtree $T_{\geq 4}$ and cotree T_4 to class $[22 \cdot 2^{3 \cdot 4}]_{288 \cdot 2^{3 \cdot 4}} = [90112]_{1179648}$.

The leftward function L in the composite function $LU^{j=2,4,6,\dots}$ (3.12) generates the upward congruence classes $[c27]_{288}$. The composite function $LU^{j=2,4,6,\dots}$ therefore generates 27 cotree congruence classes $[c27 \cdot 2^{3j}]_{288 \cdot 2^{3j}}$. The multiplication of $c27$ with 2^{3j} means that each of the 27 classes is multiplied with 2^{3j} . Since the number of congruence classes remains 27, the density decay factor $r = 1/2^{3 \cdot 2} = 1/64$ leads to fast density decay. The cumulative density of all even upward cotrees is just $1/672$.

The LCMp's of *upward* subtrees and cotrees follow from the periodicity expansions $\theta_{U1} = 2^4$ for a single (first) upward iteration U^1 (Def.5.1), and $\theta_{U2} = 2^{3 \cdot 2}$ for two upward iterations U^2 . After each further pair of two upward iterations, the number of different congruence classes remains unaltered.

The classes of subtrees and cotrees (Def.5.9) follow from the congruence classes $T_{\geq 0}[c27, c5]_{288}$ of the 27 leftward branching classes $c27$ and the 5 upward branching classes $c5$ (Def.1-2, Table 2). Since every pair of two successive upward iterations gives expansions $U^2 : n \rightarrow n \cdot 2^{3 \cdot 2}$ by $2^{3 \cdot 2}$ (Def.1), an even number of upward iterations j gives expansions by 2^{3j} . This is true for all numbers in the 27 leftward classes $c27$ and for all numbers in the 5 upward classes $c5$. This is denoted by $T_{\geq j=2,4,6,\dots} [c27 \cdot 2^{3j}, c5 \cdot 2^{3j}]_{288 \cdot 2^{3j}}$.

Definition 5.9. *Congruence classes and density even upward cotrees T_2, T_4, T_6, \dots (Fig.4d, ...)*

$$\begin{aligned}
 & U^{j=2,4,6,\dots} : T_{\geq 0} \left[\begin{array}{c} c27 \\ c5 \end{array} \right]_{288} \rightarrow \\
 & T_{\geq j} \left[\begin{array}{c} U^j(c27) \\ U^j(c5) \end{array} \right]_{288 \cdot 2^{3j}} = \\
 & T_{\geq j} \left[\begin{array}{c} c27 \cdot 2^{3j} \\ c5 \cdot 2^{3j} \end{array} \right]_{288 \cdot 2^{3j}} \\
 & LU^{j=2,4,6,\dots} : T_{\geq 0} \rightarrow T_j [c27 \cdot 2^{3j}]_{288 \cdot 2^{3j}} \\
 & d(T_2) = 27/(288 \cdot 2^{3 \cdot 2}) = 27/18432; \theta_{U2} = 2^{3 \cdot 2} \\
 & d(T_2, T_4, T_6, \dots) = a/(1-r) = d(T_2)/(1-(1/\theta_{U2})) \doteq 1/672
 \end{aligned}$$

The congruence classes of even upward cotrees are obtained by LU^j walks of tree $T_{\geq 0}$. This preserves the classes $T_j[c27 \cdot 2^{3j}]_{288 \cdot 2^{3j}}$ in cotree T_j .

Odd upward subtrees and cotrees

The congruence classes of odd upward subtrees and cotrees follow from the congruence classes in tree $T_{\geq 0}$, split up in $T_{\geq 0}[c27(15, 12), c5(1, 4)]_{288}$ in the 27 leftward branching classes $c27(15, 12)$ and the 5 upward branching classes $c5(1, 4)$ partitioned by the branching classes $[4]_{18}$ and $[16]_{18}$ (Def.5.10) This partition is shown in Table 2.

Definition 5.10. Congruence classes and density odd upward cotrees T_1, T_3, T_5, \dots (Fig.3b,3f,...)

$$\begin{aligned}
& U^{\geq k=1,3,5,\dots} : T_{\geq 0} \left[\begin{array}{c} c27(15, 12) \\ c5(1, 4) \end{array} \right]_{288} \rightarrow \\
& T_{\geq k=1,3,5,\dots} \left[\left(\begin{array}{c} c27(15, 12) \\ c5(1, 4) \end{array} \right) \vec{h}_U(4, 1) \# U^{k=1,3,5,\dots} \right]_{288 \cdot 2^{3k+1}} = \\
& T_{\geq k=1,3,5,\dots} \left[\left(\begin{array}{c} c72(60, 12) \\ c8(4, 4) \end{array} \right) \# U^{k=1,3,5,\dots} \right]_{288 \cdot 2^{3k+1}} = \\
& T_{\geq k=1,3,5,\dots} \left[\begin{array}{c} c72 \cdot 2^{3k-3} \\ c8 \cdot 2^{3k-3} \end{array} \right]_{288 \cdot 2^{3k+1}} \\
& L_{j=1,3,5,\dots} : T_{\geq j=1,3,5,\dots} \rightarrow T_j \left[c72 \cdot 2^{3k-3} \right]_{288 \cdot 2^{3k+1}} \\
& d(T_1) = 72/(288 \cdot 2^4) = 72/4096; \theta_{U2} = 2^{3 \cdot 2} \\
& d(T_1, T_3, T_5, \dots) = a/(1-r) = d(T_1)/(1 - (1/\theta_{U2})) \doteq 1/63
\end{aligned}$$

The alignment of the intrinsic periodicities to their lcm-periodicity gives for the first odd subtree $15 \cdot 4 + 12 \cdot 1 = 72$ cotree classes, denoted as $c72$ (listed in Table 2). The number 72 results from multiplying the partition of congruence classes $[c27(15, 12)]_{288}$ by the branching classes $[4, 16]_{18}$ (Def.1) with the upward alignment vector $\vec{h}_U = [4, 1]$ (Def.1). Similarly, $1 \cdot 4 + 5 \cdot 1 = 8$ nested upward congruence classes are obtained, denoted as $c8$ in Table 2.

The congruence classes themselves are obtained by applying the iterated odd upward function $U^{k=1,3,5,\dots}$ to these 72 leftward classes and 8 upward classes in the first odd subtree, denoted as $(c72(60, 12), c8(4, 4)) \# U^{k=1,3,5,\dots}$. These odd upward iterations yield the congruence classes of the first odd subtree, multiplied by $\theta_{U2} = 2^{3 \cdot 2}$ at each further iteration. Thus, the congruence classes of odd upward subtrees are $[c72 \cdot 2^{3k-3}]_{288 \cdot 2^{3k+1}}$ and $[c8 \cdot 2^{3k-3}]_{288 \cdot 2^{3k+1}}$.

The density of the first odd cotree $T_1[c72]_{288 \cdot 2^4}$, calculated as the number of congruence classes relative to their periodicity, amounts to $a = d(T_1) = 72/(288 \cdot 2^4) = 72/4096$. Together with the density decay factor $r_{U2} = 1/\theta_{U2}$ the geometric sum formula $s = a/(1-r)$ gives $1/63$ as the cumulative cotree density of all odd upward cotrees T_1, T_3, \dots (Fig.3b, Fig.3f, ...).

Leftward subtrees and cotrees

The leftward function is defined on subclasses with a periodicity three times greater than for the upward function. The first leftward walk of the tree $T_{\geq 0}[c27(15, 12), c5(1, 4)]_{288}$ assumes a periodicity of $3 \cdot 288$ instead of 288. The argument subclasses in the triple-expanded argument period are denoted as $3c27(15, 12, 15, 12, 15, 12)$ and $3c5(1, 4, 1, 4, 1, 4)$ (Def.7), where the bracketed numbers indicate the argument distribution over the six argument subclasses $[4, 16, 22, 34, 40, 52]_{54}$ of the leftward function (Def.2).

Multiplying the leftward alignment vector $\vec{h}_L = [4, 2, 1, 8, 4, 8]$ with the counts of the argument subclasses aligns the intrinsic periodicities of the six leftward argument subclasses to their lcm-periodicity. For the first leftward walk $L : T_{\geq i} \rightarrow t_{0;\geq 1}$ this multiplication would give:

$$t_{0;\geq 1} \left[\left(\begin{array}{c} c351(60, 24, 15, 96, 60, 96) \\ c81(4, 8, 1, 32, 4, 32) \end{array} \right) \cdot T \right]_{288 \cdot 2^4}$$

An additional transformation is required to obtain subclasses with a triple-expanded periodicity for the next leftward iteration. Figure 10 shows that the first four subclasses $[4, 16, 22, 34]_{54}$ have paths to the

argument subclasses $[4, 22, 40]_{54}$ of $[4]_{18}$. The subclasses $[40, 52]_{54}$ have paths to the argument subclasses $[16, 34, 52]_{54}$ of $[16]_{18}$, as illustrated in the Supplementary Materials, Fig.7-8. These path continuations are found by matrix multiplication with the transformation matrix T . Its first four rows, corresponding to the first four subclasses $[4, 16, 22, 34]_{54}$, are 1, 0, 1, 0, 1, 0 rows. They indicate the existence of paths to the first subclass $[4]_{54}$, the third subclass $[22]_{54}$ and the fifth subclass $[40]_{52}$. Its last two rows, corresponding to the last two subclasses $[40, 52]_{54}$, are 0, 1, 0, 1, 0, 1 rows. They indicate the existence of paths to the second subclass $[16]_{54}$, the fourth subclass $[34]_{54}$ and the last subclass $[52]_{54}$. This matrix multiplication gives the argument subclasses in the first leftward subtree;

$$t_{0;\geq 1} \left[\begin{pmatrix} 3c351(195, 156, 195, 156, 195, 156), \\ 3c81(45, 36, 45, 36, 45, 36) \end{pmatrix} \right]_{3 \cdot 288 \cdot 2^4}$$

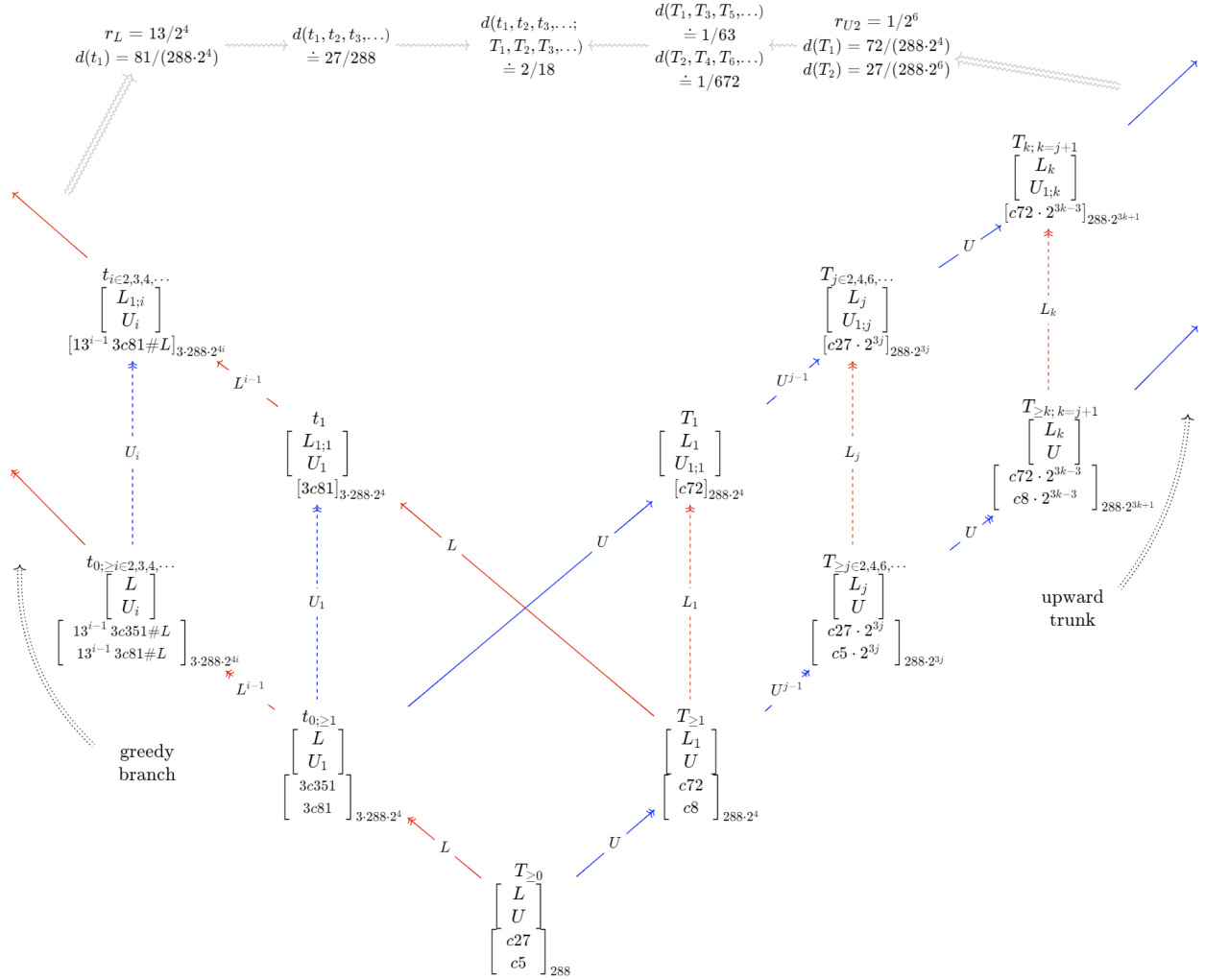
The same multiplication with \vec{h}_R and matrix multiplication by T applies to each further leftward iteration to obtain further nested leftward subtrees. Each further multiplication by the alignment vector \vec{h}_R followed by matrix multiplication by T results in 13 times more congruence classes. The number sign $\#L$ followed by the leftward function (Fig.10, Def.4, Def.7) indicates that the $13^{i-1} \cdot 3 \cdot 351 + 13^{i-1} \cdot 3 \cdot 81$ subclasses in the leftward subtree $t_{0;\geq i}$ are obtained by applying the leftward function L to previous leftward subtree $t_{0;\geq i-1}$, which holds only $13^{i-2} \cdot 3 \cdot 351 + 13^{i-2} \cdot 3 \cdot 81$ different congruence classes.

The congruence classes of leftward cotrees t_i , for $i = 1, 2, 3, \dots$, are obtained by a conjugative leftward walk L_i of subtree $t_{0;\geq i}$, or equivalently by $L^i U_i \asymp U L^i$ walks of tree $T_{\geq 0}$. The classes $t_i [13^{i-1} 3c81 \#L]_{3 \cdot 288 \cdot 2^{4i}}$ in cotree t_i are preserved, while the classes $[13^{i-1} 3c351 \#L]_{3 \cdot 288 \cdot 2^{4i}}$ are excluded.

Definition 5.11. Density leftward cotrees t_1, t_2, t_3, \dots (Figs.2bdf...)

$$\begin{aligned} L_{i=1,2,3,\dots}: T_{\geq 0} \left[\begin{pmatrix} 3c27(15, 12, 15, 12, 15, 12), \\ 3c5(1, 4, 1, 4, 1, 4) \end{pmatrix} \right]_{3 \cdot 288} &\rightarrow \\ t_{0;\geq i=1,2,3,\dots} \left[\begin{pmatrix} 3c27(15, 12, 15, 12, 15, 12), \\ 3c5(1, 4, 1, 4, 1, 4) \end{pmatrix} \right] \vec{h}_L(4, 2, 1, 8, 4, 8) \cdot T &\Big|_{288 \cdot 2^{3i+1}} = \\ t_{0;\geq i=1,2,3,\dots} \left[13^{i-1} \begin{pmatrix} 3c351(195, 156, 195, 156, 195, 156), \\ 3c81(45, 36, 45, 36, 45, 36) \end{pmatrix} \right] \#L &\Big|_{288 \cdot 2^{3i+1}} = \\ t_{0;\geq i=1,2,3,\dots} \left[\begin{pmatrix} 13^{i-1} 3c351 \#L \\ 13^{i-1} 3c81 \#L \end{pmatrix} \right] &\Big|_{3 \cdot 288 \cdot 2^{4i}} \\ L_{i=1,2,3,\dots}: t_{0;\geq i=1,2,3,\dots} &\rightarrow \\ t_{i=1,2,3,\dots} [13^{i-1} 3c81(45, 36, 45, 36, 45, 36) \#L]_{3 \cdot 288 \cdot 2^{4i}} &= \\ t_{i=1,2,3,\dots} [13^{i-1} 3c81 \#L]_{3 \cdot 288 \cdot 2^{4i}} & \\ d(t_1) = (3 \cdot 13^{1-1} \cdot 81) / (3 \cdot 288 \cdot 2^{4 \cdot 1}) = 81/4608; \theta_L = 2^4 & \\ d(t_1, t_2, t_3, \dots) = d(t_1) / (1 - (13/(3\theta_R))) \doteq 27/288 & \end{aligned}$$

Figure 11: The automorphism graph $\text{Aut}(T_{\geq 0}, [L, U])$



Legend | Arrows vs. brackets: outer vs. inner automorphism. Red vs. blue arrows: leftward vs. upward turns. Single vs. double arrowheads (\rightarrow vs. \rightarrow or \triangleright): cotree vs subtree generation. Lowercase vs uppercase subtrees (t vs. T): leftward vs upward trees. Superscript vs. subscript, solid diagonal arrows vs. dashed vertical arrows: iterates L^i and U^j vs. conjugates L_j and U_j . Table 2 enumerates the sets of congruence classes $c27, c5, c72, c8, c351$ and $c81$ of the trees. The post-multiplication notation, e.g. $c5 \cdot 2^{3j}$, indicates that 5 congruence classes are obtained by multiplying each of the $c5$ classes by 2^{3j} (Methods). Notations like $13^{i-1} \cdot 3c81 \cdot L^{i-1}$ indicate that $13^{i-1} \cdot 3 \cdot 81$ subclasses modulo 54, to which Def.2 applies, are obtained by applying L to the previous $13^{i-2} \cdot 3 \cdot 81$ subclasses (Methods). The annotations with the cotree densities $d(t_1)$, $d(T_1)$ and $d(T_2)$, and the cotree density decay factors r_L and r_{U2} reveal the cumulative cotree density $2/18$, which is equal to that of all branching numbers $S_{\geq 0} = [4, 16]_{18}$. |

The density of the first leftward cotree t_1 is $a = d(t_1) = 81/(288 \cdot 2^4)$. The density of the i 'th leftward cotree becomes $d(t_i) = (13^{i-1} \cdot 81)/(288 \cdot 2^{4i})$. The density decay is $r_L = 13/(3 \cdot 2^4) = 13/16$. The cumulative density of numbers in leftward cotrees $d(t_1, t_2, t_3, \dots) = s = a/(1 - 13/16) = 27/288$ equals the periodic density of 27 leftward numbers in each consecutive range of 288 natural numbers.

Corollary 5.12. *The Collatz function $3n + 1$ passes the periodic density test whether all natural numbers converge to $c = 4$ (Col.2.5). The cumulative density of numbers in odd upward cotrees (1/672, Eq.5.10), even upward cotrees (1/63, Eq.5.9) and leftward cotrees (27/288, E5.11) amounts to $1/672 + 1/63 + 27/288 = 32/288 = 2/18$, which equals the periodic density $2/18$ of all branching numbers $[4, 16]_{18}$ (Eq.5.1). \square*

5.3 The automorphic automorphism graph

The automorphic automorphism graph (Fig.11) results if the, in the meanwhile familiar, functions UL^i and LU^j (Eqs.3.11, 3.12) are applied both to the nodes and to the arrows of the Cayley graph $T_{\geq 0}$ (Fig.1b), thus to both its nodes and arrows, thereby generating all nodes and arrows of the already introduced subtrees and cotrees (Figs.7,8).

The automorphism graph $\text{Aut}(T_{\geq 0}, [L, U])$ (Fig.11, Def.5.13) has therefore as nodes or Vertices, isomorphic trees (Figs.1b, 7, 8, and as Edges composite L - and U -functions connecting them (Eqs.3.15, 3.16, 3.13, 3.14). The automorphism graph 3.14 appears to be a *butterfly-shaped* graph (Fig.11). It has two *infinite wings*: one of leftward subtrees and cotrees (Fig.7) and one of upward subtrees and cotrees (Fig.8). Zassenhaus' isomorphism lemma yields a somewhat similar butterfly graph with finite wings [52].

The functions that determine the inner arrows of leftward, respectively upward, subtrees and cotrees (Figs.7,8) also determine the congruence classes of their inner nodes (Def.5.13) (next Section 5).

Definition 5.13. *Generating nodes and arrows of trees within the automorphic automorphism graph*

$$\text{Aut}(T_{\geq 0}, [U, V]) \quad (4)$$

Argument tree $T_{\geq 0}$	$T_{\geq 0}(S_{\geq 0}, [L, U])$	$S_{\geq 0} = [c27, c5]_{288}$
Leftward subtrees $t_{0;\geq i}$	$L^i: T_{\geq 0}(S_{\geq 0}, [L, U]) \rightarrow t_{0;\geq i}(s_{0;\geq i}, [L, U_i])$	$s_{0;\geq i} = [13^{i-1} (3c351, 3c81) \# L]_{3 \cdot 288 \cdot 2^{4k}}$
Leftward cotrees t_i	UL^i or $L^i U_i: T_{\geq 0}(S_{\geq 0}, [L, U]) \rightarrow t_i(s_i, [L, U_i])$	$s_i = [13^{i-1} 3c81 \# L]_{3 \cdot 288 \cdot 2^{4k}}$
Upward subtrees $T_{\geq j}$	$U_0^j: T_{\geq 0}(S_{\geq 0}, [L, U]) \rightarrow T_{\geq j}(S_{\geq j}, [L_j, U])$	$S_{\geq j \in 2,4,6,\dots} = [(c27, c5) \cdot 2^{3j}]_{288 \cdot 2^{3j}}$ $S_{\geq k; k=j-1} = [(c72, c8) \cdot 2^{3k-3}]_{288 \cdot 2^{3k+1}}$
Upward cotrees T_j	LU^j or $U^j L_j: T_{\geq 0}(S_{\geq 0}, [L, U]) \rightarrow T_j(S_j, [L_j, U_1^j])$	$S_{j \in 2,4,6,\dots} = [c27 \cdot 2^{3j}]_{288 \cdot 2^{3j}}$ $S_{k=j-1} = [c72 \cdot 2^{3k-3}]_{288 \cdot 2^{3k+1}}$
Conjugate arrows:	$L_j = U^{-j} L U^j$ $L_{1;i} = L^{-i} U_1 L^i$	$U_i = L^i U L^{-i}$ $U_{1;j} = U^{-j} L_1 U^j$
Notational equivalencies	$L \asymp L^1 \asymp L_0 \asymp L_0^1, U \asymp U^1 \asymp U_0 \asymp U_0^1$	

The functions to obtain from tree $T_{\geq 0}$ the automorphism graph $\text{Aut}(T_{\geq 0}, [L, U])$ can be applied recursively to each cotree in it, yielding for each cotree a butterfly graph with two infinite wings of subtrees and cotrees, ad infinitum. Thus, each column of breadth-first ordered root paths of a cotree is placed not only in a column on the left page or right page of the middle pages graph, but also in the gutter of another pair of pages.

Table 3: Pretest whether $an + b$ function yields 1 graph component with trivial root $c = a + b$

Function $an \pm b$	$3n - 1$	$5n + 1$	$3n + 1$	$7n \pm 1$
a	3	5	3	7
b	-1	+1	+1	± 1
m argument periodicity	2	2	2	4
odd classes not divisible by a , periodicity am	$[1,5]_6$	$[1,3,7,9]_{10}$	$[1,5]_6$	$\begin{bmatrix} 1,3,5,9, \\ 11,13,15,17, \\ 19,23,25,27 \end{bmatrix}_{28}$
# odd classes not divisible by a $(a - 1)(m/2)$	2	4	2	12
Branching classes $S_{\geq 0}$, periodicity a^2m	$[2,14]_{18}$	$[6,16,36,46]_{50}$	$[4,16]_{18}$	$\begin{bmatrix} 8,36,64,92, \\ 120,176,2076, \\ 104,132,160,188 \end{bmatrix}_{196}$
Density branching classes $d(S_{\geq 0})$ $(a - 1)/(2a^2)$	2/18 (= 1/9)	4/50 (= 2/25)	2/18 (= 1/9)	12/196 (= 3/49)
Branching subclasses, periodicity a^3m	$\begin{bmatrix} 2,14,20, \\ 32,38,50 \end{bmatrix}_{54}$	$\begin{bmatrix} 6,16,36, \dots \\ \dots, 236,246 \end{bmatrix}_{250}$	$\begin{bmatrix} 4,16,22, \\ 34,40,52 \end{bmatrix}_{54}$	$\begin{bmatrix} 8,36,64, \dots \\ \dots, 1352,1364 \end{bmatrix}_{1372}$
# Branching subclasses $a(a - 1)(m/2)$	6	20	6	84
Root class subclasses, pretest numbers	$[2,20,38]_{54}$	$\begin{bmatrix} 6,56,106, \\ 156,206 \end{bmatrix}_{250}$	$[4,22,40]_{54}$	$\begin{bmatrix} 8,204,400,596, \\ 792,988,1184 \end{bmatrix}_{1372}$
Pretest numbers \rightarrow $c = a + b$?	20,38 \rightarrow 2?	56,106, 156,206 \rightarrow 6?	22,40 \rightarrow 4?	204,400,596, 792,988,1184 \rightarrow 8?
Pass root class connectivity pretest	no	no	yes	yes
Disjoint upward and rightward branching classes			$[c2 \cdot 2^l]_{18 \cdot 2^q} =$ $[c32]_{288} =$ $[c27, c5]_{288}$	$[c12 \cdot 2^l]_{196 \cdot q} =$ $[c1536]_{25088} =$ $[c1372, c164]_{25088}$

Legend | Four periodicity expansions are at the heart of Table 3. First, the argument periodicity is expanded from m to am to exclude odd classes divisible by a , which are $[3]_6, [5]_{10}, [3]_6$, respectively $[7, 21]_{28}$. The classes divisible by a have no branching successors, as successors $a \cdot 2^p$ cannot branch by $(n \pm b)/a$. Applying $an \pm b$ to the argument classes with periodicity am gives the periodicity of branching numbers a^2m . To let the leftward function $L : n \rightarrow (n \pm b)/a \cdot 2^q$ reach integer odd classes after $(n \pm b)/a$ the periodicity of branching classes a^2m (Def.5.1) increases to the periodicity a^3m of branching subclasses (Def.5.2). This is for $3n + 1$ the increase of the argument periodicity of the upward function of $a^2m = 18$ to the argument periodicity of the leftward function $a^3m = 54$. The pretest is whether the lowest numbers of the subclasses of the root class can walk to the trivial root $c = a + b$. If not, then they are part of a different graph component. $3n + 1$ and $7n \pm 1$ pass the test. The last row shows their number of leftward and upward classes and periodicities: $288 = 2^5 \cdot 3^2$, respectively $25088 = 2^9 \cdot 7^2$. |

5.4 Trivial root convergence pretest showing decidability of $an+b$ conjectures

The already announced decidability test (Theorem 1.4) is that an $an+b$ function converging for branching numbers $[n]_{2a^2}$ lower than $2a^3$ to the trivial root number $c = a + b$ will converge to it for all branching numbers (Col.5.14). The calculations in Table 3 show that the example functions $3n-1$ and $5n-1$ do not lead all their branching numbers to the trivial root $c = a + b$, in contrast with the Collatz function $3n+1$ [1] and the Bařina function $7n \pm 1$ [53]. The $7n \pm 1$ function prescribes, next to the subfunction $g^{-1} : n \rightarrow n/2$ for even numbers, the subfunctions $f^{-1} : n \rightarrow 7n+1$ for congruence class $[1]_4$ and $f^{-1} : n \rightarrow 7n-1$ for congruence class $[3]_4$.

Corollary 5.14. *Whether an $an+b$ function converges to $c = a+b$ for all branching numbers $[n]_{2a^2}$ higher than $2a^3$ depends on whether all branching numbers lower than $2a^3$ converge to $c = a + b$. Whether a branching number is connected to the trivial root $c = a + b$ determines whether its leftward and upward successors are connected to it. For example, the $3n-1$ function with branching numbers $[2, 14]_{18}$ does not connect branching number 20 lower than $2 \cdot 3^3 = 54$ to $c = a + b = 2$. Therefore the upward successors of 20, which are the branching numbers 320, 1280, 20480, \dots higher than $2a^3 = 54$ are not connected to $c = a + b$ either. Conversely, if an $an+b$ function connects all branching numbers lower than $2a^3$ to $c = a + b$, then all their successor numbers are connected to it. For such an $an+b$ function, for example for $3n+1$ and $7n \pm 1$, each branching number is a V-foot number of which the V-arm number are stretched to a row in the middle pages graph (Fig.9). (Col.5.12). For such a function, the cumulative density of cotrees, breadth-first ordered in middle page graph columns connected to $c = a + b$, equals the total density of branching numbers \square*

Corollary 5.14 implies also that, if all branching numbers $[n]_{2a^2}$ lower than $2a^3$ are connected to the trivial root $c = a + b$, then there is no root trajectory of an unconnected graph component with a perhaps colossally high lowest number X . This is proven separately (Col.5.15), exemplified by the $3n+1$ function.

Corollary 5.15. *The $an+b$ functions that converge for all branching number $[n]_{2a^2}$ lower than $2a^3$ to $c = a + b$ cannot generate also numbers in the root trajectory of a different graph component with a perhaps colossally high lowest number X . Each root trajectory number in a hypothetical root trajectory with a perhaps colossally high lowest number X of a graph component unconnected from $c = 4$ would have to be connected exclusively with still higher upward and leftward successors. These successors would have a long contracting path to the numbers in the hypothetical root trajectory with a perhaps colossally high lowest number X . Fig.10 shows that for the Collatz function $3n+1$ the contracting elementary cyclic trajectory $[16]_{18} \rightarrow [17]_{18} \rightarrow [16]_{18}$ is the only contracting cycle that can give contracting paths of arbitrary length k . However, contracting paths of arbitrary length k generated by the Collatz $3n+1$ function have as first argument number $a_k = (3^k - 1)54 + 52$ and as last output number $o_k = (2^k - 1)54 + 52$. For $k = 1, 2, 3, \dots$ the argument-output pairs are $1 : 160 \rightarrow 106, 2 : 484 \rightarrow 214, 3 : 1456 \rightarrow 430, \dots$. Since $2^{k+1} < 3^k$ for $k \geq 2$, the output of the contracting path is lower than the argument of the next longer contracting path ($484 > 106, 1556 > 214, \dots$). Thus, contracting paths of arbitrary length k generated by $3n+1$ cannot reach the numbers in an unconnected root trajectory with a colossally high number X . \square*

6 Discussion

Following its proposer [1], the proof of the Collatz conjecture combines elementary graph theory with elementary number theory. As noted by Lagarias, the conjecture is not an isolated problem [54]. Its proof suggests new cross-connections, for example to anti-symmetric ladder operators in physics (Remark 3.2). The automorphism graph (Fig.11) suggests new insights into the infinite *unfoldings* and *reinterpretations* of the world, as faintly familiar from the disjoint or nested worlds in politics, journalism, and literature according to a variety of quoted, paraphrased, observed or imagined agents.

Acknowledgments The authors are grateful for all comments and questions on earlier drafts. Especially those of former co-author Mustafa Aydogan, David Bařina, Wan Fokkink, Jan-Willem Klop, Ronald Meester, Klaas Sikkel, Eldar Sultanow, and Wouter van Attevelde, provided worthwhile hints for the revisions. We thank Christian Koch for implementing the binary Collatz tree in a Github repository (<https://github.com/c4ristian/collatz>). The article draws on sequence explorations using the Online Encyclopedia of Integer Sequences [5], commutative plots enabled by Quiver [55], and the wide variety of simulations and plots enabled by Mathematica [56].

References

- [1] L. Collatz, “On the motivation and origin of the $(3n + 1)$ -problem,” in *The Ultimate Challenge: The $3x + 1$ Problem* (J. C. Lagarias, ed.), (Providence, Rhode Island), pp. 241–248, American Mathematical Society, 2010.
- [2] D. R. Hofstadter, *Gödel, Escher, Bach: an eternal golden braid*. New York: Basic Books, 1980.
- [3] E. Roosendaal, *On the $3x + 1$ problem*. <http://www.ericr.nl/wondrous/>, Last update at the time of writing: November 11, 2023.
- [4] R. Diestel, *Graph theory* (5th ed.), vol. 173 of *Graduate texts in mathematics*. New York: Springer, 2017.
- [5] OEIS Inc, “The Online Encyclopedia of Integer Sequences.” <https://oeis.org>.
- [6] H. Ehrig, “Introduction to the algebraic theory of graph grammars,” in *Graph-Grammars and Their Application to Computer Science and Biology: International Workshop Bad Honnef, October 30–November 3, 1978* 1, pp. 1–69, Springer, 1979.
- [7] M. Dehn, “Über unendliche diskontinuierliche Gruppen,” *Mathematische Annalen*, vol. 71, no. 1, pp. 116–144, 1911.
- [8] E. W. Weisstein, “Geometric dual graph,” <https://mathworld.wolfram.com/>, 2000.
- [9] R. Overbeek and J. Endrullis, “Patch graph rewriting,” in *Graph Transformation* (F. Gadducci and T. Kehrer, eds.), (Cham), pp. 128–145, Springer International Publishing, 2020.
- [10] R. Overbeek, *A Unifying Theory for Graph Transformation*. 2024.
- [11] J. C. Lagarias, *The Ultimate Challenge: The $3x + 1$ Problem*. Rhode Island: AMS Bookstore, 2010.
- [12] A. Turing, “On computable numbers, with an application to the Entscheidungsproblem,” *Journal of Mathematics*, vol. 58, no. 345–363, p. 5, 1936.
- [13] C. A. R. Hoare and D. C. S. Allison, “Incomputability,” *ACM Computing Surveys (CSUR)*, vol. 4, no. 3, pp. 169–178, 1972.
- [14] D.-A. German, “The golden mean shift is the set of $3x + 1$ itineraries,” in *Internet: <http://www.wolframscience.com/conference/2004/presentations/material/adriangerman.pdf>*, 2004.
- [15] J. W. Klop, “Staircase to syracuse,” pp. 1–7, 2004.
- [16] A. Rahn, E. Sultanow, M. Henkel, S. Ghosh, and I. J. Aberkane, “An algorithm for linearizing the Collatz convergence,” *Mathematics*, vol. 9, no. 16, p. 1898, 2021.
- [17] T. Tao, “Almost all orbits of the Collatz map attain almost bounded values,” *Forum of Mathematics, Pi*, vol. 10, p. e10, 2022.
- [18] Veritasium, *The Simplest Math Problem No One Can Solve - Collatz Conjecture, interview with A.V. Kontorovich*. <https://www.youtube.com/watch?v=094y1Z2wpJg>, 2021.
- [19] A. V. Kontorovich and J. C. Lagarias, “Stochastic models for the $3x + 1$ and $5x + 1$ problems and related problems,” in *The Ultimate Challenge: The $3x + 1$ Problem* (J. C. Lagarias, ed.), (Providence, Rhode Island), pp. 131–188, AMS, 2010.
- [20] J. H. Conway, *Unpredictable iterations*, pp. 219–223. Providence, Rhode Island: AMS, 2010.
- [21] J. Endrullis, C. Grabmayer, and D. Hendriks, “Complexity of Fractran and productivity,” in *International Conference on Automated Deduction*, pp. 371–387, Springer, 2009.
- [22] D. Bařina, “Convergence verification of the Collatz problem,” *The Journal of Supercomputing*, vol. 77, no. 3, pp. 2681–2688, 2021.
- [23] K. R. Popper, “Logik der forschung,” 1934.
- [24] M. Aigner and G. M. Ziegler, *Proofs from the Book, 6th Ed*. Berlin: Springer, 1999.
- [25] J. C. Lagarias, “The $3x + 1$ problem: An annotated bibliography, ii (2000–2009),” *arXiv preprint math/0608208.pdf*, v6, 2010.

- [26] K. Hartnett, “Mathematician Terence Tao cracks a ‘dangerous’ problem,” *Science Wired*, vol. Dec.1, no. 15, 2019.
- [27] E. Sultanow, C. Koch, and S. Cox, *Collatz Sequences in the Light of Graph Theory*. <https://doi.org/10.25932/publishup-43008>, <https://github.com/c4ristian/collatz>, 2020.
- [28] M. Van Steen, *Graph theory and complex networks*, vol. 144. Amsterdam: Van Steen, 2010.
- [29] N. L. Biggs, *Algebraic graph theory, 2nd ed.* Cambridge: Cambridge University Press, 1996.
- [30] M. H. Weissman, *An illustrated theory of numbers*. Providence: American Mathematical Society, 2017.
- [31] N. L. Biggs, *Discrete Mathematics*. Oxford / New York: Oxford University Press, 2nd ed., 2009.
- [32] N. L. Biggs, E. K. Lloyd, and R. J. Wilson, *Graph Theory, 1736-1936*. Oxford: Oxford University Press, 1986.
- [33] J. Petersen, “Die Theorie der regulären Graphs,” *Acta Mathematica*, vol. 15, pp. 193–220, 1891.
- [34] L. Euler, *Solutio problematis ad geometriam situs pertinentis [The solution of a problem relating to the geometry of sites]*, book section 1, pp. 3–8. Oxford: Clarendon Press, 1736.
- [35] E. W. Weisstein, “Breadth-first traversal,” <https://mathworld.wolfram.com/>, 2000.
- [36] E. W. Weisstein, “Depth-first traversal,” <https://mathworld.wolfram.com/>, 2000.
- [37] W. Lenzen, “Leibniz and the calculus ratiocinator,” *Technology and Mathematics: Philosophical and Historical Investigations*, pp. 47–78, 2018.
- [38] A. M. Brunner and S. Sidki, “On the automorphism group of the one-rooted binary tree,” *Journal of Algebra*, vol. 195, no. 2, pp. 465–486, 1997.
- [39] R. Grigorchuk and D. Savchuk, “Ergodic decomposition of group actions on rooted trees,” *Proceedings of the Steklov Institute of Mathematics*, vol. 292, pp. 94–111, 2016.
- [40] B. E. Nucinkis and S. S. John-Green, “Quasi-automorphisms of the infinite rooted 2-edge-coloured binary tree,” *Groups, Geometry, and Dynamics*, vol. 12, no. 2, pp. 529–570, 2018.
- [41] J. Endrullis and D. Hendriks, “On periodically iterated morphisms,” in *Proceedings of the 23rd Conference on Computer Science Logic (CSL) and the 29th Symposium on Logic in Computer Science (LICS)*, pp. 1–10, 2014.
- [42] S. A. Cook, “The complexity of theorem-proving procedures,” in *Proceedings of the 3rd Annual ACM symposium on theory of computing*, (New York), ACM, ACM Press, 1971.
- [43] A. Cayley, “The theory of groups: graphical representation,” *American Journal of Mathematics*, vol. 1, no. 2, pp. 174–176, 1878.
- [44] B. B. Mandelbrot and M. Frame, “The canopy and shortest path in a self-contacting fractal tree,” *The Mathematical Intelligencer*, vol. 21, pp. 18–27, 1999.
- [45] L. Wittgenstein, *Tractatus logico-philosophicus*. Suhrkamp, 1921.
- [46] D. I. Spivak, *Category theory for the sciences*. Cambridge: MIT press, 2014.
- [47] S. Wolfram, *A new kind of Science*. Wolfram Inc., 2001.
- [48] E. W. Weisstein, “Isomorphic graphs,” <https://mathworld.wolfram.com/>, 2000.
- [49] E. Noether and W. Schmeidler, “Moduln in nichtkommutativen Bereichen,” *Mathematische Zeitschrift*, vol. 8, pp. 1–35, 1920.
- [50] E. W. Weisstein, “Commutative,” <https://mathworld.wolfram.com/>, 2000.
- [51] E. W. Weisstein, “Commutative diagram,” <https://mathworld.wolfram.com/>, 2000.
- [52] J. B. Fraleigh, *A first course in abstract algebra*. Pearson Education India, 2003.
- [53] D. Bařina, “ $7x \pm 1$: Close relative of Collatz problem,” *CMST Computational Methods in Science and Technology*, vol. 29, no. 4, pp. 143–147, 2022.
- [54] M. Chamberland, “A $3x + 1$ survey: Number theory and dynamical systems,” in *The Ultimate Challenge: The $3x + 1$ Problem* (J. C. Lagarias, ed.), (Providence, Rhode Island), pp. 57–78, American Mathematical Society, 2010.
- [55] N. Arkor, “quiver,” <https://github.com/varkor/quiver>, 2023.
- [56] S. Wolfram, *Mathematica: a system for doing mathematics by computer*. Addison Wesley, 1991.